N-Pyrrolyl Phosphines: An Unexploited Class of Phosphine Ligands with Exceptional π-Acceptor Character

Kenneth G. Moloy*,† and Jeffrey L. Petersen‡

Contribution from the Union Carbide Corporation, P.O. Box 8361, South Charleston, West Virginia 25303-0361, and Department of Chemistry, West Virginia University, Morgantown, West Virginia 26506-6045

Received February 28, 1995®

Abstract: The coordination chemistry of *N*-pyrrolyl phosphines (P−NC_4H_4) is described. These ligands are prepared in excellent yield from pyrrole, a phosphorus halide, and base, and this synthesis has been applied to the series PPh_x(pyrrolyl)$_{3-x}$ ($x = 0-2$) and the chelate (pyrrolyl)$_2$P$(CH_2)_2$P(pyrrolyl)$_2$. These ligands readily form coordination complexes, and the complexes *trans*-RhCl(CO)[PPh_x(pyrrolyl)$_{3-x}$]$_2$ ($x = 0-2$) and Mo(CO)$_4$[(pyrrolyl)$_2$P$(CH_2)_2$-P(pyrrolyl)$_2$] are described. The carbonyl stretching frequencies of these complexes are shifted to significantly higher energy relative to "traditional" phosphine ligands, indicating that *N*-pyrrolyl phosphines are poor σ-donors, exceeding phosphites and approaching fluoroalkylphosphines with respect to this property. For example, ν_{CO} for *trans*-RhCl(CO)-[P(pyrrolyl)$_3$]$_2$ exceeds that of the PPh_3 analogue by 59 cm^{-1}. That these ligands are π-acceptors is suggested by the single crystal X-ray structure of *trans*-RhCl(CO)[P(pyrrolyl)$_3$]$_2$ which shows shortened Rh−P distances and a lengthened Rh−C distance, consistent with enhanced Rh to P back-bonding. The X-ray structure of *trans*-RhCl(CO)-[P(pyrrolidinyl)$_3$]$_2$ is also reported; this complex possesses longer Rh−P distances which more closely resemble those found for other complexes of this type. The exceptional π-acceptor character of these ligands is convincingly demonstrated by their substitution chemistry with electron rich [PPN][Rh(CO)$_4$]. P(pyrrolyl)$_3$ is found to displace CO in a stepwise manner to give the entire series [PPN][Rh(CO)$_{4-x}${P(pyrrolyl)$_3$}$_x$] ($x = 1-4$). Similar results are obtained with (pyrrolyl)$_2$P$(CH_2)_2$P(pyrrolyl)$_2$, and the anions [PPN][Rh(CO)$_x${(pyrrolyl)$_2$P$(CH_2)_2$P(pyrrolyl)$_2$}$_y$] ($x = 2$, $y = 1$; $x = 0$, $y = 2$) are reported. An X-ray structure analysis of [PPN][Rh(CO){P(pyrrolyl)$_3$}$_3$] shows that the Rh−P bonds in this tetrahedral anion are shorter than those found in the Rh(I) complex, consistent with significantly greater π back-bonding in this more electron rich system. The infrared spectra of these anions again show a substantial shift in ν_{CO} to higher frequency relative to other phosphine ligands. The structural results further indicate that PPh_x(pyrrolyl)$_{3-x}$ ($x = 0-2$), PPh_3, and P(pyrrolidinyl)$_3$ possess nearly identical steric properties (cone angles). The wide range of electronic properties (π-acceptor/σ-donor) exhibited by this isosteric series, together with their ready availability, suggests that they, and *N*-pyrrolyl phosphines in particular, may find utility in physical inorganic and organometallic chemistry.

Introduction

Phosphorus(III) ligands of the type PZ_3, where Z is a substituent such as hydrocarbyl, alkoxy, halo, etc., are ubiquitous in coordination chemistry, organometallic chemistry, and homogeneous catalysis.[1] The wide variety of Z groups available allows the systematic alteration of ligand steric and electronic (σ-donor, π-acceptor) properties. This allows a great deal of leverage in fine tuning the reactivity of metal complexes of these ligands. It is for this reason that these ligands find such enormous and important utility.

PZ_3 ligands can, depending on the choice of Z, possess a significant degree of π-acceptor character. However, the number of such ligands approaching the π-acceptor ability of another ubiquitous ligand, CO, is rather small. This has been the subject of several recent reports, where significant effort has been expended on the chemistry of fluoroalkyl phosphines.[2] Electronically these ligands are, as might be expected, poor σ-donors and in several examples possess π-acceptor properties approaching that of CO. Their π-acceptor ability is significantly greater than that found for other phosphorus ligands known to have enhanced π-acceptor properties, such as phosphites (Z = OR).

Fluoroalkyl phosphines are not without drawbacks, however. The syntheses of these ligands are generally multistep and often involved, requiring the generation of the appropriate fluoroalkyllithium reagents[2a-e] or P(II) ($(R_f)_2PP(R_f)_2$)[2f] precursors. The scope of fluoroalkyl phosphines, as a general class, is limited due to the low variety of the appropriate R_f precursors that are

* Author to whom correspondence should be addressed. Current address: E. I. du Pont de Nemours and Company, Central Research and Development, Experimental Station E328/215A, P.O. Box 80328, Wilmington, DE 19880-0328. Email: moloykg@esvax.dnet.dupont.com.

† Union Carbide Corporation.

‡ West Virginia University.

® Abstract published in *Advance ACS Abstracts,* July 1, 1995.

(1) See the following and references therein: (a) Wilson, M. R.; Woska, D. C.; Prock, A.; Giering, W. P. *Organometallics* **1993**, *12*, 1742. (b) Caffery, M. L.; Brown, T. L. *Inorg. Chem.* **1991**, *30*, 3907. (c) Dunne, B. J.; Morris, R. B.; Orpen, A. G. *J. Chem. Soc., Dalton Trans.* **1991**, 653. (d) Corbridge, D. E. C. *Phosphorus. An Outline of its Chemistry, Biochemistry and Technology*, 4th ed.; Elsevier: New York, 1990. (e) Levason, W. In *The Chemistry of Organophosphorus Compounds*; Hartley, F. R., Ed.; Wiley: New York, 1990; Vol. 1, Chapter 15. (f) McCauliffe, C. A. *Comprehensive Coordination Chemistry*; Wilkinson, G., Gillard, R. D., McCleverty, J. A., Eds.; Pergamon: Oxford, 1987; Vol. 2, p 989. (g) Collman, J. P.; Hegedus, L. S.; Norton, J. R.; Finke, R. G. *Principles and Applications of Organotransition Metal Chemistry*; University Science Books: Mill Valley, CA, 1987; p 66. (h) *Homogeneous Catalysis with Metal Phosphine Complexes*; Pignolet, L. H., Ed.; Plenum: New York, 1983. (i) Alyea, E. C.; Meek, D. W. *Adv. Chem. Ser.* **1982**, *196*. (j) Tolman, C. A.*Chem. Rev.* **1977**, *77*, 313.

(2) (a) Schnabel, R. C.; Roddick, D. M. *Inorg. Chem.* **1993**, *32*. 1513. (b) Ernst, M. F.; Roddick, D. M. *Organometallics* **1990**, *9*, 1586. (c) Ernst, M. F.; Roddick, D. M. *Inorg. Chem.* **1989**, *28*, 1624 (d) Koola, J. D.; Roddick, D. M. *J. Am. Chem. Soc.* **1991**, *113*, 1450. (e) Brookhart, M.; Chandler, W. A.; Pfister, A. C.; Santini, C. C.; White, P. S. *Organometallics* **1992**, 11, 1263. (f) Phillips, I. G.; Ball, R. G.; Cavell, R. G. *Inorg. Chem.* **1988**, *27*, 4038.

0002-7863/95/1517-7696$09.00/0 © 1995 American Chemical Society

readily available (e.g., the preparation of R_fLi necessitates access to the R_fI or R_fCl precursor[2a-e]). This also places limits on the ability to methodically evaluate ligand steric and electronic factors on the chemistry of metal complexes of these ligands by systematic alteration of the fluoroalkyl group R_f.

We sought to enter this particular area of phosphorus ligand chemistry by seeking an alternative class of ligands which would obviate the drawbacks noted for fluoralkyl phosphines. To this end, a previous study by Drago *et al.*,[3] on the coordination chemistry of pyrrolyldithiocarbamate, was noted. In particular, a comparison of the oxidation potentials for the complexes $Fe(S_2CNR_2)_3$ is very informative. For NR_2 = pyrrolyl, the electrochemistry shows that the oxidation potentials of complexes of this ligand are dramatically increased. As shown in Table 1, the oxidation potential for the *N*-pyrrolyl derivative is *ca.* 0.7 V greater than that for the corresponding pyrrolidinyl (with a saturated ring) dithiocarbamate. The introduction of this unsaturated, aromatic heterocycle greatly increases the ease with which an electron can be added to the metal and significantly stabilizes lower oxidation states.

The explanation proposed[3] for this observation follows. The best resonance representation for simple dithiocarbamate (R = CH_3, CH_2CH_3, $(CH_2)_4$, etc., in **A** and **B**, below) ligands involves a significant degree of electron donation from nitrogen to carbon (**B**). It is for this reason that these ligands tend to be good donors. In the case of NR_2 = pyrrolyl, however, this electron donation is disrupted due to aromatic delocalization of the nitrogen lone pair into the five-membered ring, and the best resonance contribution for this ligand is given by **D**. The net effect is that the aromaticity of the pyrrolyl ring renders it a powerful electron withdrawing group relative to other NR_2 moieties. For the dithiocarbamate derivative, this results in greatly reduced σ-donor ability and enhanced π-acidity (this latter conclusion is reached from a consideration of other properties of Fe(pyrroledtc)$_3$ as determined by magnetism and Mössbauer spectroscopy studies[3]).

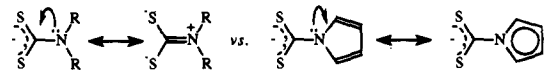

A **B** **C** **D**

The dramatic influence of the pyrrolyl group on dithiocarbamate coordination chemistry caused us to consider if an analogous influence could be achieved with the *N*-pyrrolyl phosphines. A similar series of resonance forms can be drawn for these ligands which suggest that *N*-pyrrolyl phosphines should be relatively weak σ-donors and possibly good π-acceptors. Qualitatively, aromatic delocalization of the nitrogen lone pair into the ring might have the following benefits: Any N → P π-donation (**E**) is eliminated, and a partial positive charge is placed adjacent to phosphorus (**G** and **H**). The aromatic resonance form **I** would also be expected to act in an electron withdrawing fashion relative to the phenyl groups in a ligand such as PPh_3 because carbon has been replaced with a more electronegative nitrogen atom.

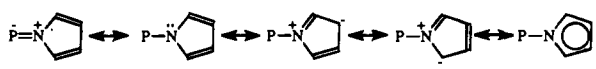

E **F** **G** **H** **I**

A perusal of the literature suggests that this class of ligands has merit in this regard. P(pyrrolyl)$_3$ and several related compounds have been reported previously[4] and are readily prepared by treatment of the appropriate phosphorus halide with an alkali metal pyrrolide (MNC_4H_4). The reactivity of these compounds is in fact unusual when compared to that for simple tris(dialkylamino)phosphines or tris(hydrocarbyl)phosphines. For instance, P(pyrrolyl)$_3$ does not react with CH_3OH and, in fact, can be recrystallized from that solvent.[4a] In contrast, ordinary tris(dialkylamino)phosphines readily react with alcohols to liberate free amine with concomitant formation of the corresponding phosphite.[1d] P(pyrrolyl)$_3$ also fails to react with CH_3I.[4a] This observation should be contrasted with the reactivity of tris(hydrocarbyl)phosphines, such as PPh_3 and $P(CH_3)_3$, which are rapidly quaternized by CH_3I to give the phosphonium salts $[R_3PCH_3][I]$.[1d] These observations are consistent with a greatly reduced nucleophilicity for phosphorus in P(pyrrolyl)$_3$,[4a] as might be anticipated by a consideration of the resonance structures shown above. This behavior is reminiscent of that found for fluoroalkyl phosphines and other phosphines with weak σ-donor ability.[2] These observations, in addition to the lack of reports on transition metal complexes of *N*-pyrrolyl phosphines,[5] caused us to initiate a study on the coordination chemistry of these potentially very interesting ligands, in addition to an evaluation of their σ-donor/π-acceptor properties. This report describes these efforts and includes improved synthetic procedures, coordination chemistry, spectroscopy, and structural investigations. These results are used to contrast the ligand properties of *N*-pyrrolyl phosphines with classical tris(hydrocarbyl)phosphines and also tris(dialkylamino)phosphines.

Table 1. Oxidation Potentials (V vs Ag/AgCl) for Iron Tris(dithiocarbamates) (from Ref 3)

		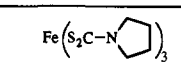
Fe^{2+}/Fe^{3+}	−0.3	+0.3
Fe^{3+}/Fe^{4+}	+0.6	+1.3

Results and Discussion

Ligand Syntheses. The previously reported syntheses of *N*-pyrrolyl phosphines were accomplished by reaction of alkali metal pyrrolides, such as KNC_4H_4, with the appropriate phosphorus chloride.[4] Although the reported yields were in general quite good, this procedure consistently gave only mediocre results in our hands. Yields were lower than expected (50−60%), and the products were often contaminated, as determined by ^{31}P NMR, with small amounts of unidentified products which were difficult to remove by recrystallization. A significantly improved route to the parent compound P(pyrrolyl)$_3$ is the direct reaction of pyrrole with PCl_3 in the presence of Et_3N, as shown by the generic reaction in eq 1. Heating these reagents overnight in THF is sufficient to give complete reaction and clean conversion to P(pyrrolyl)$_3$. Monitoring the reaction

(3) El A'mma, A. G.; Drago, R. S. *Inorg. Chem.* **1977**, *16*, 2975.

(4) (a) Fischer, S.; Hoyano, J.; Johnson, I.; Peterson, L. K. *Can. J. Chem.* **1976**, *54*, 2706. (b) Mrowca, J. J. U.S. 3,816,452, 1974. (c) Gurevich, P. A.; Kiselev, V. V.; Moskva, V. V.; Malsyutova, S. F.; Zykova, T. V. *Zh. Obsch. Khim.* **1983**, *53*, 238. (d) Marschner, F.; Kessel, H.; Goetz, H. *Phosphorus* **1976**, *6*, 135. (e) Issleib, K.; Brack, A. *Z. Anorg. Allg. Chem.* **1957**, *292*, 245.

(5) Only one previous[5a] report exists of a metal complex of P(pyrrolyl)$_3$ or a related ligand. The main topic of this article, however, is a comparison of the solid state structures of P(pyrrolyl)$_3$ and Sb(pyrrolyl)$_3$. Only brief mention is made of the reaction of P(pyrrolyl)$_3$ with $Fe_2(CO)_9$ to yield $Fe(CO)_4[P(pyrrolyl)_3]$. The infrared spectrum of this complex was not reported. Only a single reference in the patent literature describing the use of these ligands has been located. P(pyrrolyl)$_3$ and related compounds have been reported as useful promoters in the nickel-catalyzed coupling of 1,3-dienes with ethylene to give 1,4-hexadienes.[5b] (a) Atwood, J. L.; Cowley, A. H.; Hunter, W. E.; Mehrota, S. K. *Inorg. Chem.* **1982**, *21*, 1354. (b) Cramer, R. D. U.S. 4,028,429, 1977.

by ^{31}P NMR shows that the reaction proceeds sequentially, and all intermediates of the type $PCl_x(pyrrolyl)_{3-x}$ ($x = 1-3$) can be observed during the course of the reaction. The product is readily purified by vacuum sublimation at 50−80 °C and 10−50 μ Hg or by crystallization from cold hexane.

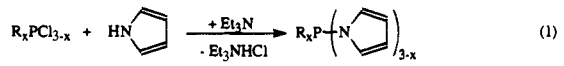

(1)

This route has been found to be suitable for a number of *N*-pyrrolyl phosphine compounds. Thus, we successfully used this method to prepare the entire series $PPh_x(pyrrolyl)_{3-x}$ ($x = 0-2$). Starting with commercially available $Cl_2P(CH_2)_2PCl_2$ we also prepared the diphosphine $(pyrrolyl)_2P(CH_2)_2P(pyrrolyl)_2$ for comparison with the classic chelating ligand DIPHOS ($Ph_2P(CH_2)_2PPh_2$). P(pyrrolidinyl)$_3$ was prepared by the same general procedure shown in eq 1, using pyrrolidine and PCl_3, in order to better gauge the impact of the aromatic heterocycle on the coordination chemistry of substituted tris(amino) phosphines.[6]

These ligands exhibit the expected NMR spectral features with the possible exception of the ^{31}P NMR line widths, which are generally broad. For instance, the ^{31}P line width for P(pyrrolyl)$_3$ is *ca.* 64 Hz (25 °C, toluene-d_8). The line widths are presumably influenced by the quadrupolar nitrogen nucleus and should be compared with the more typical *ca.* 5 Hz line width we observe for a compound such as PPh_3. This broadening serves as a useful diagnostic tool which indicates formation of *N*-bonded product.

Coordination Chemistry: Complexes with Rh(I) and Mo(0). A study of the chemistry of these ligands with transition metals was next undertaken. Specifically, we sought to prepare and study metal carbonyl complexes of these ligands. Infrared spectroscopy (ν_{CO}) could then be used to gauge the donor effects of *N*-pyrrolyl phosphines and also to make comparisons with other phosphorus(III) ligands.[7] We first chose to investigate the complexes *trans*-$RhCl(CO)(PR_3)_2$. $[RhCl(CO)_2]_2$ reacts with phosphines quantitatively and rapidly (minutes) at room temperature to give these square planar Rh(I) complexes (eq 2).[8] The presence of a single carbonyl ligand results in a simple infrared spectrum which is readily interpreted. Generation of $RhCl(CO)(PR_3)_2$ complexes may thus be used as a rapid "spot test" of the donor properties of new ligands. This attribute has been recognized for many years and an extensive literature exists for these complexes,[8,9] allowing ready comparison with a variety of other phosphorus(III) ligands. The use of ν_{CO} in these complexes to evaluate ligand electronic properties has also been long recognized and used as a gauge of the electron density at rhodium[10] and the effect of ligand electronics on reactivity,[11] including catalysis.[12]

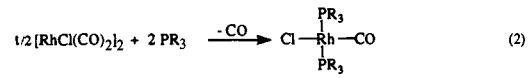

(2)

As expected, *N*-pyrrolyl phosphines readily form coordination complexes with rhodium; addition of these ligands to $[RhCl(CO)_2]_2$ results in rapid CO evolution and formation of the desired *trans*-$RhCl(CO)(PR_3)_2$ complexes. These reactions may be followed by infrared spectroscopy, discussed in further detail below, which shows clean and nearly instantaneous conversion of the dimeric starting material to product.[13]

While all of the monodentate ligands we report here form carbonyl complexes of this type, an attempt to synthesize the chelate complex *cis*-$[RhCl(CO)\{(pyrrolyl)_2P(CH_2)_2P(pyrrolyl)_2\}]$ by this method failed, and a complex approximating $[RhCl\{(pyrrolyl)_2P(CH_2)_2P(pyrrolyl)_2\}]_2$ is isolated instead. Similar behavior has been reported[2a] with dfepe $(C_2F_5)_2P(CH_2)_2P(C_2F_5)_2$, a weak σ-donor/good π-acceptor ligand. Thus, RhCl(CO)(dfepe) can be generated from $[RhCl(dfepe)]_2$ in the presence of CO but cannot be isolated due to the high lability of the carbonyl ligand and resulting reversion to the chloro-bridged dimer. We were, however, able to successfully prepare and isolate the complex $Mo(CO)_4\{(pyrrolyl)_2P(CH_2)_2P(pyrrolyl)_2\}$ by reaction of the chelate with $Mo(CO)_6$ (eq 3). This complex is isolated in good yield as colorless crystals from toluene.

$$Mo(CO)_6 + (pyrrolyl)_2P(CH_2)_2P(pyrrolyl)_2 \xrightarrow{-2CO} Mo(CO)_4\{(pyrrolyl)_2P(CH_2)_2P(pyrrolyl)_2\} \quad (3)$$

The infrared spectra of the *trans*-$RhCl(CO)(PR_3)_2$ complexes demonstrate that the *N*-pyrrolyl group acts as a potent electron withdrawing group and that *N*-pyrrolyl phosphines are indeed weak σ-donor ligands. As shown in Table 2A, the carbonyl frequencies are significantly higher than those found for trialkyl and triaryl phosphines, and, in some cases, phosphites. For instance, the CO stretch is shifted to higher energy by nearly 60 cm^{-1} upon substitution of PPh_3 by P(pyrrolyl)$_3$. A comparison of the available data[2c] for the *cis* chelate complexes $Mo(CO)_4P_2$ (Table 2B) further exemplifies this point. It is also interesting to compare the IR data obtained for the series of ligands $PPh_x(pyrrolyl)_{3-x}$. Spectral data for the rhodium complexes of this ligand series are depicted graphically in Figure 1, showing a steady, monotonic increase in ν_{CO} with increasing degree of replacement of phenyl with *N*-pyrrolyl. This series of essentially isosteric ligands (*vide infra*) spans a 60 cm^{-1} range in *ca.* 20 cm^{-1} increments, showing that the *N*-pyrrolyl group

(6) P(pyrrolidinyl)$_3$ has also been prepared *via* reaction of pyrrolidine with $P(NEt_2)_3$: Hussain, L. A.; Elias, A. J.; Rao, M. N. S. *Tetrahedron Lett.* **1988**, *29*, 5983.

(7) Poulton, J. T.; Sigalas, M. P.; Folting, K.; Streib, W. E.; Eisenstein, O.; Caulton, K. G. *Inorg. Chem.* **1994**, *33*, 1476.

(8) (a) Evans, D.; Osborn, J. A.; Wilkinson, G. *Inorg. Synth.* **1990**, *28*, 79. (b) Franks, S.; Hartley, F. R. *Inorg. Chim. Acta* **1981**, *47*, 235. (c) Intille, G. M. *Inorg. Chem.* **1972**, *11*, 695. (d) Deeming, A. J.; Shaw, B. L. *J. Chem. Soc. A* **1969**, 597. (e) McCleverty, J. A.; Wilkinson, G. *Inorg. Synth.* **1966**, *8*, 214.

(9) Hughes, R. P. *Comprehensive Organometallic Chemistry*; Wilkinson, G., Stone, F. G. A., Abel, A., Eds.; Pergamon Press: Oxford, 1982; Chapter 35, p 296ff.

(10) (a) Ohgomori, Y.; Yoshida, S.; Watanabe, Y. *J. Chem. Soc., Dalton Trans.* **1987**, 2969. (b) de Montauzon, D.; Poilblanc, R. *J. Organomet. Chem.* **1975**, *93*, 397.

(11) Sakakura, T.; Sodeyama, T.l Sasaki, K. Wada, K.; Tanaka, M. *J. Am. Chem. Soc.* **1990**, *112*, 7221

(12) (a) Kopylova, L. I.; Pukhnarevich, V. B.; Tsykhanskaya, I. I.; Satsuk, E. N.; Timokhin, B. V.; Dmitriev, V. I.; Chvalovsky, V.; Capka, M.; Kalabina, A. V.; Voronkov, M. G. *Zh. Obshch. Khim.* **1981**, *51*, 1851. (b) Grimbolt, J.; Bonnelle, J. P.; Mortreux, A.; Petit, F. *Inorg. Chim. Acta* **1979**, *34*, 29. (c) Unverferth, K.; Rueger, C.; Schwetlick, K. *J. Prakt. Chem.* **1977**, *319*, 841. (d) Vastag, S.; Heil. B.; Markó, L. J. *Mol. Catal.* **1979**, *5*, 189. (e) Yoshikawa, S.; Kiji, J.; Furukawa, J. *Makromol. Chem.* **1977**, *178*, 1077. (f) Strohmeier, W.; Rehder-Stirnweiss, W. *Z. Naturforsch. B* **1971**, *26*, 61. (g) Strohmeier. W.; Rehder-Stirnweiss, W. *Z. Naturforsch. B* **1970**, *25*, 549. (h) Strohmeier, W.; Rehder-Stirnweiss, W. *J. Organomet. Chem.* **1969**, *19*, 417. (i) Strohmeier. W.; Rehder-Stirnweiss, W. *J. Organomet. Chem.* **1969**, *18*, 28.

(13) ^{31}P NMR spectroscopy of these reaction solutions shows that rapid (NMR time scale) exchange occurs between coordinated ligand and any excess ligand present in solution. The resulting ^{31}P NMR spectra generally show exchange broadened resonances exhibiting no coupling between rhodium and phosphorus and chemical shifts intermediate between those of the complex and free ligand. Isolation of the pure complexes as yellow crystals, free of any excess ligand, is readily achieved by crystallization from warm toluene. The complexes thus purified show sharp resonances with the expected chemical shifts and rhodium−phosphorus coupling. Thus, while the formation of these complexes may a useful spot test with respect to IR spectroscopy, its use for *in situ* NMR spectroscopy is limited.

Table 2. Metal Carbonyl Stretching Frequencies for Rh(I) and Mo(0) Complexes

ligand	ν_{CO} (cm^{-1})	ref
A. *trans*-RhCl(CO)L_2		
$P(pyrrolyl)_3$	2024[a]	this work
$PhP(pyrrolyl)_2$	2007[a]	this work
$Ph_2P(pyrrolyl)$	1992[a]	this work
$P(OPh)_3$	2016[a]	12d
$P(p\text{-}CF_3C_6H_4)_3$	1990[a]	this work
PPh_3	1965[b]	14, 15
$P(CH_3)_3$	1960[b]	16
P^nBu_3	1955[b]	8b
$P(pyrrolidinyl)_3$	1952[a]	this work
B. $Mo(CO)_4(P^{\cap}P)$[c]		
$(pyrl)_2P(CH_2)_2(pyrl)_2$	2043	this work
$(C_6F_5)_2P(CH_2)_2(C_6F_5)_2$	2041	2c
$(C_2F_5)_2P(CH_2)_2(C_2F_5)_2$	2064	2c
$Ph_2P(CH_2)_2PPh_2$	2020	2c

[a] CH_2Cl_2. [b] Nujol. [c] Only the CO stretch for the high frequency, A_1 symmetry band for these C_{2v} complexes is listed; spectra for the Mo(0) complexes recorded as Nujol mulls.

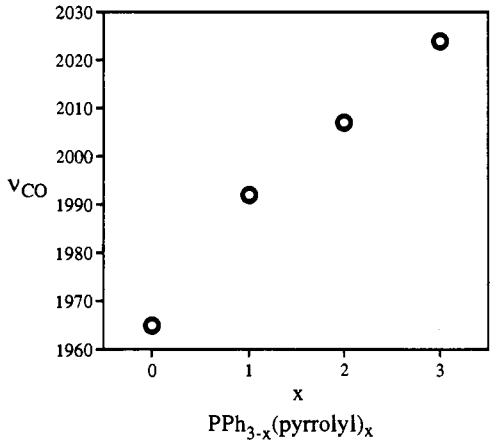

Figure 1. Graphic showing the steady increase in ν_{CO} upon substitution of Ph with *N*-pyrrolyl in the series of complexes *trans*-RhCl(CO)-$[PPh_{3-x}(pyrrolyl)_x]_2$ ($x = 0-3$).

can be used in a systematic fashion to adjust the phosphorus donor properties and, in turn, electron density at the metal center. Systematic evaluations of PR_3 ligand effects are often conducted with ligands of constant cone angle in order to eliminate the potential confounding influences of steric effects.[1a] It is for this reason that ligands of the type $P(p\text{-}XC_6H_4)_3$ find such utility in physical inorganic and organometallic chemistry. For comparison with the ligands described herein, note that ν_{CO} for the complex $RhCl(CO)[P(p\text{-}CF_3C_6H_4)_3]_2$ is 1990 cm^{-1}, slightly less than that achieved upon replacement of a single phenyl group in PPh_3 with *N*-pyrrolyl (cf., $RhCl(CO)[PPh_2(pyrrolyl)]_2$, ν_{CO} = 1992 cm^{-1}).

Using the reported correlation[12d] between the CO stretching frequencies for $RhCl(CO)(PR_3)_2$ and $Ni(CO)_3(PR_3)$ (A_1 band) we estimate ν_{CO} for $Ni(CO)_3[P(pyrrolyl)_3]$ to be *ca.* 2092 cm^{-1}. From this value it can be further estimated that the electronic parameter χ for $P(pyrrolyl)_3$ is 36, and therefore the substituent contribution χ_i for the *N*-pyrrolyl group is *ca.* 12.[1j]

These shifts to higher frequency indicate a significantly reduced degree of donation of e^- density from rhodium to the carbonyl ligand in both the Rh(I) and Mo(0) complexes and thereby indicates a reduced σ-donor ability and/or greater π-acceptor character for $P(pyrrolyl)_3$ and other members of this family of ligands. These results are all the more dramatic by noting that for the rhodium complexes these ligands are *cis* to the carbonyl, where such electronic effects are relatively minor

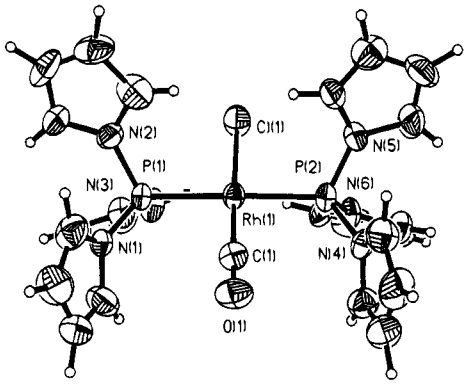

Figure 2. ORTEP drawing of *trans*-$RhCl(CO)[P(pyrrolyl)_3]_2$ (molecule 1). Thermal ellipsoids are drawn at the 50% probability level.

when compared to situations where a phosphine and carbonyl are in mutally *trans* arrangements.

Finally, the IR data for these *N*-pyrrolyl phosphine complexes should also be compared with those found for more typical tris-(dialkylamino) phosphines. The CO stretching frequency for $RhCl(CO)\{P(pyrrolidinyl)_3\}_2$ is 1952 cm^{-1} (Table 2A) and that for the $P(N(CH_3)_2)_3$ analogue is reported[17] to be 1959 cm^{-1}. Thus, the simple tris(dialkylamino) phosphines are seen to be potent donor ligands,[18] of the same magnitude as basic tris-(alkyl) phosphines such as P^nBu_3 ($\nu_{CO} \approx 1965-1950$ cm^{-1} for $RhCl(CO)[P(alkyl)_3]_2$[9]). This is interesting because it might be expected that the electronic properties of tris(dialkylamino) phosphines would fall between those of tris(alkyl) phosphines and phosphites. This is clearly not the case and may be attributed to the ability of nitrogen to engage in π-bonding with phosphorus *via* a resonance form similar to that discussed above (**E**). The potent donor properties of tris(dialkylamino)phosphines further exemplifies the powerful electron withdrawing effect of the aromatic *N*-pyrrolyl functionality.

Structural Studies of $RhCl(CO)\{P(NR_2)_3\}_2$ Complexes. I. Molecular Structure of $RhCl(CO)[P(pyrrolyl)_3]_2$. In order to further explore the steric and electronic properties of these ligands and also to gain further insight into *N*-pyrrolyl phosphines as a general class, the structure of $RhCl(CO)[P(pyrrolyl)_3]_2$ was investigated by X-ray crystallography.

A view of the complex is shown in Figure 2. The unit cell

(14) Dunbar, K. R.; Haefner, S. C. *Inorg. Chem.* **1992**, *31*, 3676.

(15) There appears to be some discrepency in the literature with respect to the CO stretching frequency for $RhCl(CO)(PPh_3)_2$. Depending on the report, this band reportedly falls in the range 1980−1975 or 1965−1960 cm^{-1}, a significant difference. This has been attributed to the presence of *cis* (high frequency) and *trans* (low frequency) isomers.[15a] Discrepancies may also arise from the complexity of the reaction of $[RhCl(CO)_2]_2$ with nonstoichiometric amounts of phosphine.[9] In our hands, CH_2Cl_2 solutions of *trans*-$RhCl(CO)(PPh_3)_2$ show a single, strong band at 1965 cm^{-1}. (a) *Organometallic Compounds of Cobalt, Rhodium, And Iridium*; White, E. Ed.; Chapman and Hall: London, 1985; p 183.

(16) Boyd, S. E.; Field, L. D.; Hambley, T. W.; Partridge, M. G. *Organometallics* **1993**, *12*, 1720.

(17) Wang, K.; Emge, T. J.; Goldman, A. S. *Organometallics* **1994**, *13*, 2135.

(18) Infrared spectra for the series of complexes *trans*-$RhCl(CO)[PPh_x(NRR')_{3-x}]_2$ ($x = 0-2$; R, R' = Et, Me; R = Me, Cy) have been reported.[12b] However, the trend reported is opposite that observed here; increasing replacement of Ph with dialkylamino is reported to result in a shift in ν_{CO} to higher frequency. No other supporting characterization information on these complexes is reported. Curiously, it is also reported that the $Ni(CO)_3[PPh_x(NRR')_{3-x}]$ derivatives show the expected trend toward lower ν_{CO}. In view of the known complex equilibria resulting from the reaction of $[RhCl(CO)_2]_2$ with nonstoichiometric amounts of ligand,[9] we believe these results are suspect and should be reinvestigated. This is supported by the reported infrared spectrum of $RhCl(CO)[P(NMe_2)_3]_2$,[17] which we have verified and shows that ν_{CO} is shifted to lower frequency relative to the PPh_3 complex. Further support is obtained from work by Vastag et al.,[12d] which shows an excellent, positive correlation between ν_{CO} values for $RhCl(CO)(PR_3)_2$ and $Ni(CO)_3(PR_3)$ complexes.

contains two crystallographically independent molecules of the complex. The molecules differ only slightly, with small changes in the relative orientations of the pyrrolyl groups about phosphorus. As expected, the complex features a square planar rhodium atom bearing *trans* phosphorus ligands. Important intramolecular bond distances and angles are given in Table 3. The two phosphine ligands adopt an eclipsed configuration, a common structural feature for these complexes. One P−N bond of each phosphorus ligand in $RhCl(CO)[P(pyrrolyl)_3]_2$ is also eclipsed with respect to the carbonyl ligand. This feature causes two of the pyrrolyl groups to effectively sandwich the carbonyl ligand and prevents a propeller-like arrangement of the pyrrolyl groups about phosphorus. An identical arrangement of substituents has been reported for the monoclinic form of $RhCl(CO)(PPh_3)_2$.[19] The energy difference between eclipsed and staggered geometries in this class of complexes is apparently small. This is evidenced by the reported[14,20] triclinic modification of $RhCl(CO)(PPh_3)_2$, where the PPh_3 ligands are found to be staggered and the phenyl groups are in the familiar propeller arrangement.

The N−P distances (av 1.69 Å) are indistinguishable from those found in the free ligand (1.70 Å).[5a] As expected, the nitrogen atoms are planar, with the sum of angles at nitrogen ranging from 356.1 to 359.9°. The bond distances within the pyrrole rings are also similar to those found in the free ligand.[5a] Thus, in the free ligand the average distances for N−C_α (1.39 Å), C_α−C_β (1.34 Å), and C_β−C_β (1.40 Å) are equivalent to those given in Table 3, within experimental error. The ligand unfolds slightly upon coordination to the RhCl(CO) fragment as shown by the sum of N−P−N angles of 306° (molecule 1) and 307° (molecule 2), which may be compared to the value of 301° found in P(pyrrolyl)$_3$. The average Rh−P−N angle is 116°. For comparison, in monoclinic $RhCl(CO)(PPh_3)_2$ the sum of C−P−C angles averages 312°, and the average Rh−P−C angle is 114.6°.[19] An exhaustive analysis[21] of A_3P−Z structures has suggested that as π back-bonding increases, the A−P−A angle generally decreases and P−A lengthens. Conversely, in a purely σ P to Z interaction the A−P−A angle increases and is accompanied by a decrease in the P−A bond length. With rhodium, and middle d-transition series metals in general, the A_3P fragment is usually little changed from that of the free ligand, such as we find for $RhCl(CO)[P(pyrrolyl)_3]_2$. This has been attributed to offsetting σ-donor and π-acceptor contributions, and this may be the case with the present example. Alternatively, it may be that the effects of Rh−P back-bonding are insufficient in the present case to result in significant ligand distortion. As seen later in this contribution, greatly enhanced back-bonding can indeed have a significant influence on ligand metrical parameters.

While the overall structural features are as expected (square planar rhodium, *trans* phosphine ligands), the bond lengths involving rhodium are of particular interest. A comparison of relevant bond lengths with a number of other *trans*-$RhCl(CO)(PR_3)_2$ structures is provided in Table 4. From these data it is seen that $RhCl(CO)[P(pyrrolyl)_3]_2$ possesses the shortest Rh−P and Rh−Cl bonds, and the longest Rh−C bond, observed for this class of complexes. Although the differences in bond lengths are small, these trends are consistent for all of the complexes $RhCl(CO)(PR_3)_2$ that have been structurally characterized, strongly suggesting a significant change in the bonding has occurred.

Table 3. Selected Interatomic Distances (Å) and Bond Angles (deg) in $Rh(CO)Cl[P(pyrrolyl)_3]_2$

A. Interatomic Distances

molecule 1		molecule 2	
Rh(1)−Cl(1)	2.351(4)	Rh(2)−Cl(2)	2.349(4)
Rh(1)−P(1)	2.288(4)	Rh(2)−P(3)	2.275(3)
Rh(1)−P(2)	2.277(4)	Rh(2)−P(4)	2.286(3)
Rh(1)−C(1)	1.866(14)	Rh(2)−C(26)	1.824(15)
P(1)−N(1)	1.697(14)	P(3)−N(7)	1.709(13)
P(1)−N(2)	1.674(13)	P(3)−N(8)	1.674(13)
P(1)−N(3)	1.687(10)	P(3)−N(9)	1.692(12)
P(2)−N(4)	1.704(12)	P(4)−N(10)	1.706(12)
P(2)−N(5)	1.681(12)	P(4)−N(11)	1.666(13)
P(2)−N(6)	1.700(12)	P(4)−N(12)	1.693(13)
O(1)−C(1)	1.114(16)	O(2)−C(26)	1.169(18)

B. Ring Bond Lengths

	molecule 1			molecule 2		
	N−C_α	C_α−C_β	C_β−C_β	N−C_α	C_α−C_β	C_β−C_β
range	1.366−1.418	1.306−1.371	1.390−1.456	1.352−1.420	1.306−1.412	1.344−1.404
average	1.387	1.339	1.414	1.387	1.358	1.376

C. Bond Angles

molecule 1		molecule 2	
Cl(1)−Rh(1)−P(1)	90.6(1)	Cl(2)−Rh(2)−P(3)	89.9(1)
Cl(1)−Rh(1)−P(2)	89.0(2)	Cl(2)−Rh(2)−P(4)	89.8(1)
P(1)−Rh(1)−P(2)	177.6(1)	P(3)−Rh(2)−P(4)	179.2(2)
Cl(1)−Rh(1)−C(1)	175.7(4)	Cl(2)−Rh(2)−C(26)	176.2(5)
P(1)−Rh(1)−C(1)	91.1(5)	P(3)−Rh(2)−C(26)	89.1(4)
P(2)−Rh(1)−C(1)	89.4(5)	P(4)−Rh(2)−C(26)	91.1(4)
Rh(1)−P(1)−N(1)	120.4(4)	Rh(2)−P(3)−N(7)	119.0(4)
Rh(1)−P(1)−N(2)	113.9(5)	Rh(2)−P(3)−N(8)	113.7(4)
N(1)−P(1)−N(2)	101.2(7)	N(7)−P(3)−N(8)	99.9(6)
Rh(1)−P(1)−N(3)	114.2(5)	Rh(2)−P(3)−N(9)	115.2(4)
N(1)−P(1)−N(3)	98.5(6)	N(7)−P(3)−N(9)	100.0(6)
N(2)−P(1)−N(3)	106.5(6)	N(8)−P(3)−N(9)	107.0(6)
Rh(1)−P(2)−N(4)	119.3(5)	Rh(2)−P(4)−N(10)	119.0(4)
Rh(1)−P(2)−N(5)	113.8(5)	Rh(2)−P(4)−N(11)	114.5(4)
N(4)−P(2)−N(5)	101.3(6)	N(10)−P(4)−N(11)	100.4(6)
Rh(1)−P(2)−N(6)	115.4(4)	Rh(2)−P(4)−N(12)	116.1(4)
N(4)−P(2)−N(6)	98.6(6)	N(10)−P(4)−N(12)	99.0(6)
N(5)−P(2)−N(6)	106.4(7)	N(11)−P(4)−N(12)	105.4(7)

The shift to short Rh−P and Rh−Cl bonds and to a long Rh−C bond is consistent with the infrared spectroscopy results. Because phosphorus in $RhCl(CO)[P(pyrrolyl)_3]_2$ is electron deficient, and hence a poor σ-donor, the structure suggests that the shortened Rh−P distance may result from enhanced π-back-bonding from rhodium to phosphorus. The poor σ-donor and good π-acceptor character of this ligand is compensated for by changes in bonding between rhodium and both chlorine and carbon. Because rhodium is unsaturated (16 e^-) in this complex, the reduced electron density at the metal is compensated for by enhanced donation of electrons from the chlorine lone pairs[27] and the Rh−Cl bond shortens as a result. The Rh−C distance

(19) Ceriotti, A.; Ciani, G.; Sironi, A. *J. Organomet. Chem.* **1983**, *247*, 345.

(20) Chaloner, P. A.; Claver, C.; Hitchcock, P. B.; Masdue, A. M.; Ruiz, A. *Acta Crystallogr.* **1991**, *C47*, 1307.

(21) (a) Dunne, B. J.; Morris, R. B.; Orpen, A. G. *J. Chem. Soc., Dalton Trans.* **1991**, 653. For further discussion see: (b) Davies, M. S.; Aroney, M. J.; Buys, I. E.; Hambley, T. W.; Calvert, J. L. *Inorg. Chem.* **1995**, *34*, 330.

(22) Monge, A.; Gutiérrez-Puebla, E.; Heras, J. V.; Pinilla, E. *Acta Cryst.* **1983**, *C39*, 446.

(23) Dahan, F.; Choukroun, R. *Acta Cryst.* **1985**, *C41*, 704.

(24) Wajda, K.; Pruchnik, F.; Lis, T. *Inorg. Chim. Acta* **1980**, *40*, 207.

(25) (a) Harlow, R. L.; Westcott, S. A.; Thorn, D. L.; Baker, R. T. *Inorg. Chem.* **1992**, *31*, 323. (b) Schumann, H.; Heisler, M.; Pickardt, J. *Chem. Ber.* **1977**, *110*, 1020.

Table 4. A Summary of Crystallographically Determined Bond Lengths for the Complexes *trans*-RhCl(CO)$(PR_3)_2$[a]

phosphine	Rh−P (Å)	ΔRh−P[b] (Å)	Rh−Cl (Å)	ΔRh−Cl[b] (Å)	Rh−C (Å)	ΔRh−C[b] (Å)	ref
P(pyrrolyl)$_3$[c]	2.282 (4)		2.350 (4)		1.845 (15)		this work
P(pyrrolidinyl)$_3$	2.333 (1)	−0.051	2.369 (1)	−0.019	1.812 (4)	+0.033	this work
PPh_3[d]	2.322 (1)	−0.040	2.382 (1)	−0.032	1.77 (1)	+0.08	14
PPh_3[d]	2.326 (1)	−0.044	2.371 (2)	−0.021	1.810 (7)	+0.035	19
PPh_3[d]	2.323 (6)	−0.041	2.414 (11)	−0.064	1.84 (2)	0	20
P(*p*-FC_6H_4)$_3$	2.322 (2)	−0.040	2.381 (2)	−0.031	1.800 (7)	+0.045	22
$P(CH_3)Ph_2$[c]	2.315 (2)	−0.033	2.362 (2)	−0.012	1.795 (2)	+0.050	23
$P(CH_3)_3$	2.308 (1)	−0.026	2.354 (1)	−0.004	1.770 (4)	+0.075	16
P(2-pyridyl)$_3$	2.298 (4)	−0.016	2.399 (7)	−0.049	1.82 (3)	+0.03	24
P^tBu_3[e]	2.428 (1)	−0.146	2.389 (2)	−0.039	1.780 (4)	+0.065	25
DMPP[f]	2.313 (8)	−0.031	2.366 (4)	−0.016	1.77 (1)	+0.08	26
DBP[g]	2.293 (1)	−0.011	2.372 (1)	−0.022	1.824 (6)	+0.021	26
$P(C_2H_3)Ph_2$	2.323 (6)	−0.041	2.479 (1)	−0.129	1.827 (8)	+0.018	26

[a] Standard deviations (in parentheses) are the simple average of the individual standard deviations for each bond length when the average of more than one bond length is listed. [b] Δ = distance$_{Rh-X}$(*trans*-RhCl(CO)[P(pyrrolyl)$_3$]$_2$) − distance$_{Rh-X}$(*trans*-RhCl(CO)$(PR_3)_2$). [c] Average values for two independent molecules in the unit cell, each with crystallographically independent *trans* phosphorus ligands. [d] Del Pra *et al.* have also reported the solid state structure of RhCl(CO)$(PPh_3)_2$. However, the determination appears to be of questionable quality. See: Del Pra, A.; Zanotti, G. *Cryst. Struct. Comm.* **1979**, *8*, 959. [e] The average values for two structures, one a toluene solvate and the other unsolvated, and each possessing crystallographically inequivalent P^tBu_3 ligands. This complex is severely congested and highly distorted from square planar geometry. [f] DMPP = 1-phenyl-3,4-dimethylphosphole. [g] DBP = 1-phenyldibenzophosphole.

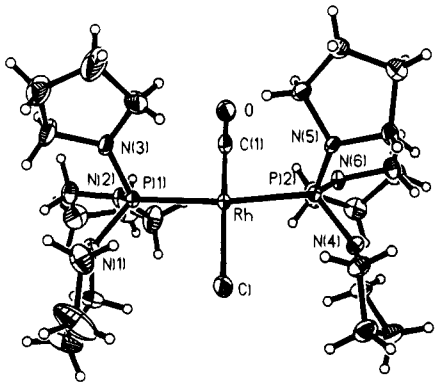

Figure 3. ORTEP drawing of *trans*-RhCl(CO)[P(pyrrolidinyl)$_3$]$_2$. Thermal ellipsoids are drawn at the 50% probability level.

lengthens due to diminished π-back-bonding to the carbonyl, which now competes with phosphorus as a π-acid.[28] The diminished carbonyl back-bonding in RhCl(CO)[P(pyrrolyl)$_3$]$_2$ is indicated by its carbonyl stretching frequency at 2024 cm^{-1}, which is significantly higher in energy than a prototypical phosphine such as PPh_3 (1965 cm^{-1}), as discussed above. The shortened Rh−P distance may also be explained by hybridization changes at phosphorus resulting from the *N*-pyrrolyl substituents. However, the further decrease in the Rh−P distance in a much more e^- rich rhodium complex (*vide infra*) is more consistent with enhanced Rh−P π back-bonding.

II. Molecular Structure of RhCl(CO)[P(pyrrolidinyl)$_3$]$_2$. The structure of the complex RhCl(CO)[P(pyrrolidinyl)$_3$]$_2$ was also determined in order to compare the structures of two related but electronically very different ligands. A drawing of the molecule is shown in Figure 3. As with RhCl(CO)[P(pyrrolyl)$_3$]$_2$, the molecule consists of a square planar rhodium center with *trans* phosphorus ligands. The molecule does not lie on a symmetry element, and the two phosphine ligands are crystallographically independent. The phosphorus ligands are again arranged in an eclipsed configuration. In this case the Rh−Cl bond is eclipsed with a P−N bond and as a result the chlorine ligand is sandwiched between two pyrrolidinyl groups. In RhCl(CO)[P(pyrrolyl)$_3$]$_2$ the carbonyl ligand was sandwiched between two heterocycles. We do not attach any significance to this result, as chlorine and carbonyl ligands are often disordered in these complexes,[14] indicating a small energy difference between these two solid state isomers. Important bond lengths and angles are given in Table 5. A comparison with other RhCl(CO)P_2 complexes can also be made by consulting Table 4, which shows that this molecule is unremarkable with respect to its structure about rhodium.

The most interesting aspect of this structure are the geometries at nitrogen. Each P(pyrrolidinyl)$_3$ ligand bears two nearly planar nitrogens (sum of angles at nitrogen = 354 to 360°) and one pyramidal nitrogen (sum of angles at nitrogen = 347, 350°). Although the structure of the free ligand has not been reported, the structures of the related tris(dialkylamino)phosphines P(*N*-piperidyl)$_3$ and P(*N*-morpholyl)$_3$ have been published.[29] Several transition metal complexes of $P(NMe_2)_3$ have also been characterized by X-ray crystallography.[30] These published structures exhibit the same phenomenon observed here for coordinated P(pyrrolidinyl)$_3$; two nitrogens are almost planar while the third is more pyramidal. Moreover, the spatial orientations of the heterocyclic substituents in these structures are also similar. Thus, the pyramidal nitrogen is oriented such that its lone pair is *anti* to the phosphorus lone pair (which, of course, is coordinated to rhodium in RhCl(CO)[P(pyrrolidinyl)$_3$]$_2$), as shown by **J**. It is the rings involving the pyramidal nitrogens which sandwich the chloride ligand. The two planar nitrogen atoms are oriented such that the nitrogen lone pair bisects the N(sp^3)−P−(Rh or lone pair) angle (**K**). The N−P bond lengths follow a pattern where the bond involving the pyramidal nitrogen is slightly longer (av 1.688 (3) Å in RhCl(CO)[P(pyrrolidinyl)$_3$]$_2$) than those involving the planar nitro-

(26) Kessler, J. M.; Nelson, J. H., Frye, J. S.; DeCian, A.; Fischer, J. *Inorg. Chem.* **1993**, *32*, 1048.

(27) Poulton, J. T.; Folting, K.; Streib, W. E.; Caulton, K. G. *Inorg. Chem.* **1992**, *31*, 3190.

(28) Complexes of the type *trans*-RhCl(CO)$(PR_3)_2$ are prone to disorder between the chlorine and carbonyl ligands.[14] Such a disorder in RhCl(CO)[P(pyrrolyl)$_3$]$_2$ would also explain the lengthened Rh−C and shortened Rh−Cl distances, although we have not yet found evidence for this possibility. However, this type of disorder in RhCl(CO)[P(pyrrolyl)$_3$]$_2$ would be expected to have little or no effect on the Rh−P distances and our conclusion regarding the demonstration of enhanced Rh−P bonding holds.

(29) (a) Rømming, C.; Songstad, J. *Acta Chem. Scand. A* **1980**, *34*, 365. (b) Rømming, C.; Songstad, J. *Acta Chem. Scand. A* **1978**, *32*, 689. For more discussion of the electronic structure of tris(dialkylamino)phosphines see the following and references therein: (c) Cowley, A. H.; Lattman, M.; Stricklen, P. M.; Verkade, J. G. *Inorg. Chem.* **1982**, *21*, 543. (d) Hargis, J. H.; Worley, S. D. *Inorg. Chem.* **1977**, *16*, 1686.

(30) (a) Xi, S. K.; Schmidt, H.; Lensink, C.; Kim, S.; Wintergrass, D.; Daniels, L. M.; Jacobson, R. A.; Verkade, J. G. *Inorg. Chem.* **1990**, *29*, 2214. (b) Hunt, J. J.; Duesler, E. N.; Paine, R. T. *J. Organomet. Chem.* **1987**, *320*, 307. (c) Socol, S. M.; Jacobson, R. A.; Verkade, J. G. *Inorg. Chem.* **1984**, *23*, 88. (d) Cowley, A. H.; Davis, R. E.; Remadna, K. *Inorg. Chem.* **1981**, *20*, 2146.

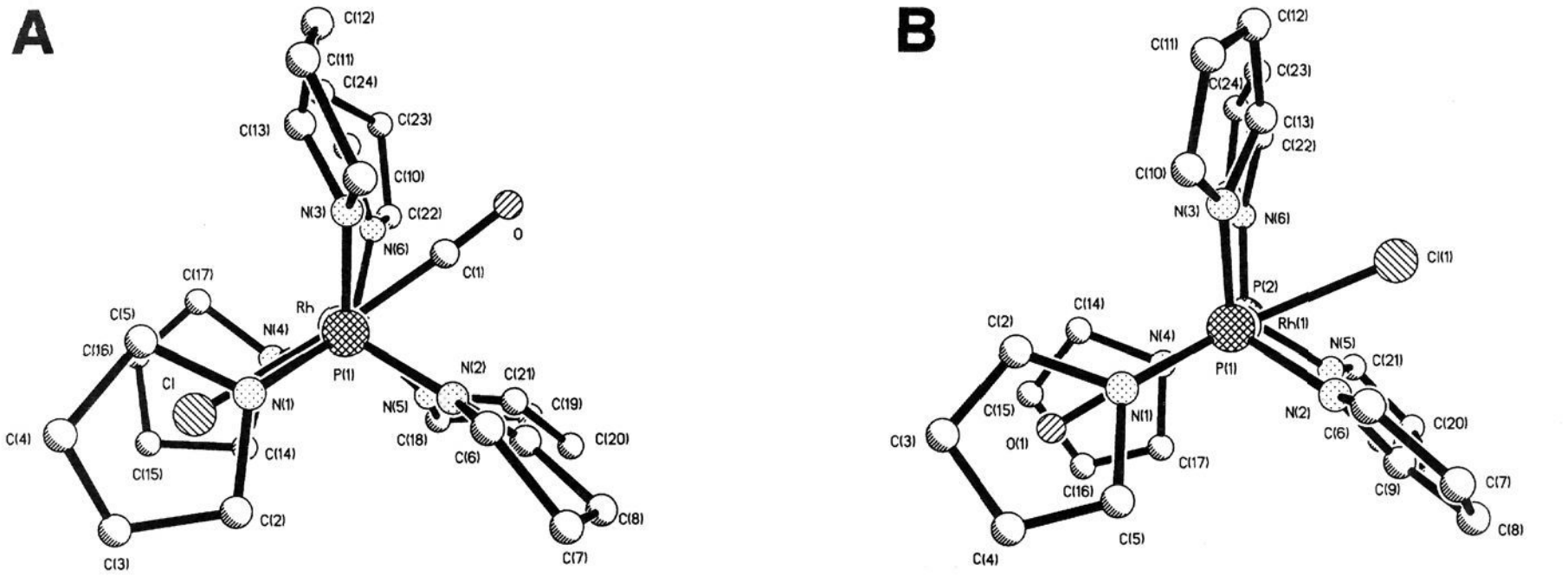

Figure 4. Comparative view of the solid state structures of *trans*-RhCl(CO)[P(pyrrolidinyl)$_3$]$_2$ (A) and *trans*-RhCl(CO)[P(pyrrolyl)$_3$]$_2$ (B), viewed down the P−Rh−P vectors and demonstrating the equivalent arrangements of the phosphorus ligands and heterocyclic substituents. Ring hydrogens have been omitted for clarity.

Table 5. Selected Interatomic Distances (Å) and Bond Angles (deg) in Rh(CO)Cl[P(pyrrolidinyl)$_3$]$_2$

	A. Interatomic Distances		
Rh−Cl	2.369(1)	Rh−P(1)	2.336(1)
Rh−P(2)	2.330(1)	Rh−C(1)	1.812(4)
P(1)−N(1)	1.688(3)	P(1)−N(2)	1.666(3)
P(1)−N(3)	1.666(3)	P(2)−N(4)	1.687(2)
P(2)−N(5)	1.667(3)	P(2)−N(6)	1.667(3)
O−C(1)	1.124(4)		
	B. Bond Angles		
Cl−Rh−P(1)	93.1(1)	Cl−Rh−P(2)	91.4(1)
P(1)−Rh−P(2)	173.4(1)	Cl−Rh−C(1)	176.4(1)
P(1)−Rh−C(1)	87.3(1)	P(2)−Rh−C(1)	88.5(1)
Rh−P(1)−N(1)	123.4(1)	Rh−P(1)−N(2)	110.9(1)
N(1)−P(1)−N(2)	100.3(2)	Rh−P(1)−N(3)	110.6(1)
N(1)−P(1)−N(3)	101.8(2)	N(2)−P(1)−N(3)	108.6(1)
Rh−P(2)−N(4)	123.5(1)	Rh−P(2)−N(5)	110.7(1)
N(4)−P(2)−N(5)	99.1(1)	Rh−P(2)−N(6)	111.0(1)
N(4)−P(2)−N(6)	102.1(2)	N(5)−P(2)−N(6)	109.2(1)
Rh−C(1)−O	177.2(4)	P(1)−N(1)−C(5)	118.8(3)
P(1)−N(1)−C(2)	119.1(2)	P(1)−N(2)−C(6)	125.7(2)
C(2)−N(1)−C(5)	109.4(3)	C(6)−N(2)−C(9)	110.0(3)
P(1)−N(2)−C(9)	124.2(3)	P(1)−N(3)−C(13)	122.8(2)
P(1)−N(3)−C(10)	124.1(3)	P(2)−N(4)−C(14)	122.3(3)
C(10)−N(3)−C(13)	109.6(3)	C(14)−N(4)−C(17)	109.8(2)
P(2)−N(4)−C(17)	117.4(2)	P(2)−N(5)−C(21)	119.5(2)
P(2)−N(5)−C(18)	125.5(2)	P(2)−N(6)−C(22)	123.1(2)
C(18)−N(5)−C(21)	109.1(2)	C(22)−N(6)−C(25)	110.3(3)
P(2)−N(6)−C(25)	123.5(3)		

gens (av 1.667 (3) Å). This bond length pattern, wherein the pyramidal nitrogen−phosphorus bond lengths exceed those involving planar nitrogen, is also observed for P(*N*-piperidyl)$_3$ and P(*N*-morpholyl)$_3$.[29a,b] The P−N bond lengths in coordinated P(pyrrolidinyl)$_3$ are uniformly shorter (by 0.03−0.04 Å) than those found in P(*N*-piperidyl)$_3$ and P(*N*-morpholyl)$_3$.

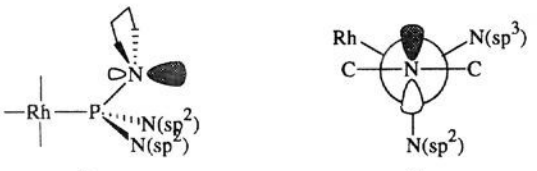

J

K

A comparison of the phosphorus ligands in the two *cis*-RhCl(CO)(PN$_3$)$_2$ structures reported here is informative. The cone angles we calculate for P(pyrrolyl)$_3$ and P(pyrrolidinyl)$_3$ in these structures are virtually identical (and equal to *ca.* 145° [31]). The relative orientations of the heterocyclic substituents on phosphorus are similar: in each structure the phosphorus ligands are mutually eclipsed, and either a carbonyl ligand (P(pyrrolyl)$_3$) or a chlorine ligand (P(pyrrolidinyl)$_3$) ligand is sandwiched between two heterocyclic rings. Figure 4 shows a comparative view of the two structures exemplifying these points. The monoclinic modification of RhCl(CO)(PPh$_3$)$_2$,[19] as described above, possesses an identical arrangement of ligands and also possesses a phosphine cone angle indistinguishable from those of the tris(amino) phosphines discussed here.[31] The steric similarity and equivalent spatial arrangements of these ligands indicates that any other differences between the two structures may be attributed to electronic effects. The bond lengths involving phosphorus and the planar sp^2-nitrogens in RhCl(CO)[P(pyrrolidinyl)$_3$]$_2$ are slightly shorter than those in RhCl(CO)[P(pyrrolyl)$_3$]$_2$. This suggests that the P−N interactions in RhCl(CO)[P(pyrrolidinyl)$_3$]$_2$ are more significant than those in RhCl(CO)[P(pyrrolyl)$_3$]$_2$, and this in turn may be attributable to π-donation from nitrogen to phosphorus. A contribution from a resonance form similar to **E**, above, may account for the planar nitrogens in RhCl(CO)[P(pyrrolidinyl)$_3$]$_2$ as well as the shortened P−N bond lengths.

It should be pointed out that empty orbitals on phosphorus are available to participate in bonding such as that depicted by **E** and that this is accompanied by enhanced phosphorus basicity. Recently, Verkade[30a,32] showed that protonation of the bicyclic tris(amino)phosphine in eq 4 yields a five-coordinate cation, where the transannular nitrogen forms a bond with phosphorus

(31) For the purposes of this study, cone angles for P(pyrrolyl)$_3$, P(pyrrolidinyl)$_3$, and PPh$_3$ were first calculated from the crystallographically determined structures of the complexes *trans*-RhCl(CO)(PR$_3$)$_2$ using the method of Tolman.[1j] The fractional coordinates were used to visualize these structures with the Molecule Editor on a CAChe Molecular Modeling System (Tektronix, Inc.), using van der Waals radii. No minimizations were performed. The crystallographically determined Rh−P bond length was used for each determination. In all cases the atom of the ligand substituents giving the largest cone angle was a hydrogen ortho to phosphorus. Because the phosphorus substituents are arranged unsymmetrically in these structures the sum of half angles was used to calculate the cone angle. From these structures we calculate virtually identical cone angles of 160°, 161°, and 160° for P(pyrrolyl)$_3$, P(pyrrolidinyl)$_3$, and PPh$_3$, respectively. The widely quoted cone angle for PPh$_3$ is 145°,[1j] derived from models wherein the phosphorus phenyl substituents are oriented so as to give the minimum cone angle. It seems entirely reasonable that the pyrrolyl and pyrrolidinyl substituents can be similarly oriented and therefore that P(pyrrolyl)$_3$ and P(pyrrolidinyl)$_3$ should also be considered to possess cone angles of 145°.

(32) Tang, J.; Dopke, J.; Verkade, J. G. *J. Am. Chem. Soc.* **1993**, *115*, 5015.

(the transannular P−N distance decreases by 1.4 Å upon protonation). The pK_a of the conjugate acid is ca. 16, which may be compared with the corresponding values for triaryl- (pK_a ≈ 3) and trialkylphosphines (pK_a ≈ 8). Clearly, this additional electron donation to phosphorus greatly enhances the basicity of this compound. A similar affect may be operative in the complex RhCl(CO)[P(pyrrolidinyl)$_3$]$_2$ as well as other complexes of tris(dialkylamino) phosphines. This would explain the infrared spectrum of RhCl(CO)[P(pyrrolidinyl)$_3$]$_2$ (and other tris(dialkylamino) phosphines) which indicates substantially increased electron density on rhodium. This is also consistent with the shorter P−N bond lengths found in coordinated P(pyrrolidinyl)$_3$ as compared to those in the structures of noncoordinated P(*N*-piperidyl)$_3$ and P(*N*-morpholyl)$_3$.

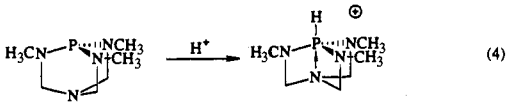

(4)

Competitive Ligand Exchange in [RhCl(CO){P(NR$_2$)$_3$}$_2$] Complexes: P(pyrrolyl)$_3$ *vs* P(pyrrolidinyl)$_3$. The single crystal structural analyses of RhCl(CO)[P(pyrrolyl)$_3$]$_2$ and RhCl(CO)[P(pyrrolidinyl)$_3$]$_2$ show that the two P(NR$_2$)$_3$ ligands have virtually identical cone angles. As a result, any differences in reactivity, etc., of metal complexes of these ligands is attributable to electronic effects. As shown by the IR spectra of their Rh(I) complexes, P(pyrrolyl)$_3$ and P(pyrrolidinyl)$_3$ are at opposite extremes of the σ-donor/π-acceptor continuum. This caused us to consider which of these ligands forms the more stable metal complexes. To begin to address this question we sought to determine to which side the equilibrium shown in eq 5 lies. Measurement of the equilibrium constant for this competition reaction would provide a quantitative measure of the preference of Rh(I) to bind an excellent σ-donor *vs* an excellent π-acceptor, without the confounding influence of steric factors.

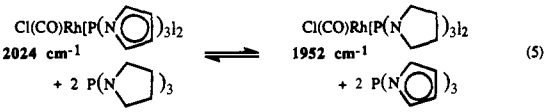

(5)

The reaction of RhCl(CO)[P(pyrrolyl)$_3$]$_2$ with P(pyrrolidinyl)$_3$ proceeds in a stepwise fashion. Addition of 1.3 equiv of P(pyrrolidinyl)$_3$ leads to complete disappearance of the 2024 cm^{-1} band in the infrared spectrum attributable to RhCl(CO)[P(pyrrolyl)$_3$]$_2$. In its place, two new bands are observed at 1988 and 1952 cm^{-1}. The latter band is due to the complex RhCl(CO)[P(pyrrolidinyl)$_3$]$_2$. Based on its position intermediate between these two complexes (indeed, exactly half way), we assign the 1988 cm^{-1} band to the mixed phosphine complex RhCl(CO)[P(pyrrolyl)$_3$][P(pyrrolidinyl)$_3$]. Addition of more P(pyrrolidinyl)$_3$ (>2 equiv total) leads to loss of the 1988 cm^{-1} band and quantitative formation of RhCl(CO)[P(pyrrolidinyl)$_3$]$_2$. Consistent with these results, a separate experiment showed that addition of P(pyrrolyl)$_3$ to RhCl(CO)[P(pyrrolidinyl)$_3$]$_2$ results in no reaction as determined by IR spectroscopy. These experiments show that the equilibrium in eq 5 lies well toward the right and that complexation with the better σ-donor ligand is greatly favored.

Similar competition experiments have been reported using the ligands P(C$_6$H$_{11}$)$_3$, PPh$_3$, and P(OPh)$_3$.[33] Although the steric properties of this series of ligands varies widely and large excesses of added ligand were employed, the same trend is observed: Rh(I) favors coordination of the more potent σ-donor ligand. The stability of the mixed ligand complexes MCl(CO)PP′ relative to a mixture of MCl(CO)P$_2$ and MCl(CO)P′$_2$ (M = Rh, Ir) has also been demonstrated previously.[34] Consistent with our assignment above, the CO stretch for these mixed ligand complexes falls between those observed for the two symmetrical species MCl(CO)P$_2$ and MCl(CO)P′$_2$.

Coordination Chemistry with Rh(−1). The results described thus far indicate that Rh(I) prefers to coordinate strong σ-donor ligands. In retrospect this result is perhaps not surprising. Because the rhodium center in the complexes *trans*-RhCl(CO)(PR$_3$)$_2$ is 16 e$^-$ and therefore unsaturated, it might have been predicted that potent σ-donor ligands would form the more stable complexes. Although some degree of metal to ligand back-bonding undoubtedly occurs in these complexes, this is apparently not a critical factor, and, therefore, π-acceptor ligands such as P(pyrrolyl)$_3$ form less stable complexes. This suggests that it might be instructive to investigate the coordination chemistry of *N*-pyrrolyl phosphines with very electron rich systems. To this end, we chose to investigate the chemistry of these ligands with a low valent, electron rich (i.e., saturated, 18 e$^-$), anionic metal center. Complexes of this type strongly prefer ligands with π-acceptor character, and for this reason the coordination chemistry of complexes falling in this category is dominated by ligands such as CO, e.g., M(CO)$_x^{y-}$.

We chose to investigate the substitution chemistry of [Rh(CO)$_4$]$^-$. By maintaining a rhodium center a better comparison can be made with the results obtained with the 16 e$^-$ Rh(I) system described above. There is also sufficient experimental evidence with [Rh(CO)$_4$]$^-$ which shows that, as expected, phosphines do not compete well with CO for coordination to this highly electron rich metal center. Chan reports[35] that sodium amalgam reduction of RhCl(CO)(PR$_3$)$_2$ (PR$_3$ = PPh$_3$, PPh$_2$CH$_3$, PPh(CH$_3$)$_2$, P(CH$_3$)$_3$) under 1 atm CO leads to exclusive formation of [Rh(CO)$_4$]$^-$. Only when the resulting solution is purged with nitrogen to remove CO does substitution occur. With typical phosphines such as PPh$_3$ and P(CH$_3$)$_3$ only a single CO ligand is substituted, resulting in formation of the tricarbonyl anions [Rh(CO)$_3$(PR$_3$)]$^-$. If a phosphorus ligand with enhanced π-acceptor character is employed, such as P(OPh)$_3$, amalgam reduction of the corresponding complex *trans*-RhCl(CO)P$_2$ under 1 atm CO gives a mixture of [Rh(CO)$_4$]$^-$ and [Rh(CO)$_3$(P(OPh)$_3$)]$^-$. Purging this solution with nitrogen leads to gradual formation of the dicarbonyl anion [Rh(CO)$_2$-{P(OPh)$_3$}$_2$]$^-$. Two carbonyl ligands may also be displaced in the case of the chelating ligand Ph$_2$P(CH$_2$)$_2$PPh$_2$ to give [Rh(CO)$_2${Ph$_2$P(CH$_2$)$_2$PPh$_2$}]$^-$.

The anions [Rh(CO)(PPh$_3$)$_3$]$^-$ and [Rh(CO)$_2$(PPh$_3$)$_2$]$^-$ (as the Bu$_4$N$^+$ salts) have been reported by other researchers.[36] The monocarbonyl was generated by electrochemical reduction of [Rh(CO)(PPh$_3$)$_3$][ClO$_4$]. This anion was characterized by *in situ* IR as well as by its reaction with CO to first give [Rh(CO)$_2$(PPh$_3$)$_2$]$^-$, also characterized by *in situ* IR, and then [Rh(CO)$_3$(PPh$_3$)]$^-$. In a related observation, Chan[35c] showed that placing the complex [Rh(CO)$_3$(PPh$_3$)]$^-$ under CO leads to complete phosphine displacement and regeneration of [Rh(CO)$_4$]$^-$. Finally, the only homoleptic phosphine complex in this series to have been reported is [Rh(PF$_3$)$_4$]$^-$, which was prepared by

(33) Strohmeier, W.; Rehder-Stirnweiss, W.; Reischig, G. *J. Organomet. Chem.* **1971**, *17*, 393.

(34) Garrou, P. E.; Hartwell, G. E. *Inorg. Chem.* **1976**, *15*, 646.

(35) (a) Chan, A. S. C. *Inorg. Chim. Acta* **1993**, *210*, 5. (b) Chan, A. S. C.; Shieh, H. -S.; Hill, J. R. *J. Organomet. Chem.* **1985**, *279*, 171. (c) Chan, A. S. C.; Carroll, W. E.; Willis, D. E. *J. Mol. Catal.* **1983**, *19*, 377.

(36) (a) Zotti, G.; Zecchin, S.; Pilloni, G. *J. Organomet. Chem.* **1983**, *246*, 61. (b) Pilloni, G.; Zotti, G.; Martelli, M. *Inorg. Chim. Acta* **1975**, *13*, 213.

Scheme 1. Titration of [PPN][Rh(CO)$_4$] with P(pyrrolyl)$_3$

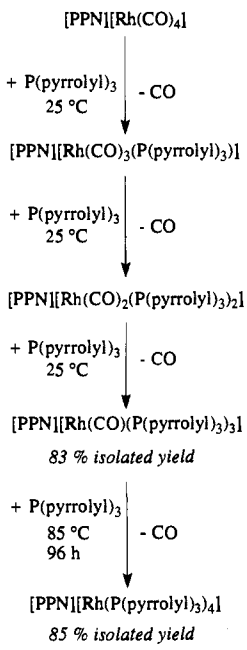

deprotonation of HRh(PF$_3$)$_4$.[37] PF$_3$, of course, is known to possess electronic properties resembling those of CO.[38] These results adequately demonstrate that anionic, 18 e$^-$ rhodium(−1) strongly prefers to coordinate ligands with very good π-acceptor character; indeed, ligands approaching the electronic properties of CO are required. The substitution chemistry of [Rh(CO)$_4$]$^-$ would therefore appear to be a good test of the π-acceptor properties of P(pyrrolyl)$_3$ and other members of this family.

To this end, [PPN][Rh(CO)$_4$] was titrated with P(pyrrolyl)$_3$; a summary of the reaction sequence is provided in Scheme 1. Addition of 1 equiv of P(pyrrolyl)$_3$ to this starting material in THF solution leads to immediate gas evolution. Spectroscopic monitoring shows disappearance of [Rh(CO)$_4$]$^-$ (1895 cm^{-1}) and clean formation of a new species. The IR spectrum shows two new bands at 1970 and 1900 cm^{-1}, and the ^{31}P NMR spectrum shows, in addition to a resonance attributable to PPN$^+$, a single doublet (spectral data are summarized in Table 6). We assign this new species as the tricarbonyl [Rh(CO)$_3$(P(pyrrolyl)$_3$)]$^-$. Addition of a second equivalent of P(pyrrolyl)$_3$ to this solution leads to disappearance of the two bands attributed to the tricarbonyl and formation of two new bands at 1943 and 1897 cm^{-1}. This is also accompanied by the appearance of a second doublet in the ^{31}P NMR spectrum. This transformation is quantitative as determined by these spectroscopic methods, and the data are entirely consistent with substitution of a second carbonyl ligand and formation of [Rh(CO)$_2$(P(pyrrolyl)$_3$)$_2$]$^-$.

Reaction with a third equivalent of P(pyrrolyl)$_3$ leads to gradual collapse of the IR bands assigned to [Rh(CO)$_2$(P(pyrrolyl)$_3$)$_2$]$^-$ and the appearance of a single absorption at 1919 cm^{-1}. This transformation may also be followed by ^{31}P NMR which shows quantitative formation of a third Rh−P(pyrrolyl)$_3$ complex, again as a doublet. These observations are clearly consistent with the formation of the *monocarbonyl* [Rh(CO)(P(pyrrolyl)$_3$)$_3$]$^-$. Indeed, this complex can be crystallized and isolated in 83% yield as the THF adduct [PPN][Rh(CO){P(pyrrolyl)$_3$}$_3$]·C$_4$H$_8$O.

(37) Kruck, T.; Lang, W.; Derner, N.; Stadler, M. *Chem. Ber.* **1968**, *101*, 3816.

(38) Cotton, F. A.; Wilkinson, G. *Advanced Inorganic Chemistry*; Wiley: New York, 1988, p. 64.

Further substitution chemistry underscores the unusual properties of this class of ligands. Reaction of [PPN][Rh(CO){P(pyrrolyl)$_3$}$_3$] with excess P(pyrrolyl)$_3$ at elevated temperature leads to gradual CO evolution and quantitative formation of a fourth Rh−P(pyrrolyl)$_3$ complex. The IR spectrum shows a complete loss of CO ligands. A single doublet is observed in the ^{31}P NMR spectrum with a chemical shift and J_{Rh-P} similar to those observed for the anionic Rh−P(pyrrolyl)$_3$ complexes previously described. Consistent with the ^{31}P spectrum, the ^{1}H NMR shows only resonances due to a single pyrrolyl moiety. Integration of the ^{31}P and ^{1}H spectra shows that the ratio of coordinated P(pyrrolyl)$_3$ to PPN$^+$ is 4:1. Based on these data this new complex is assigned to the homoleptic phosphine anion [PPN][Rh{P(pyrrolyl)$_3$}$_4$]. This complex is readily isolated as crystals in 85% yield from Et$_2$O/THF as the THF monosolvate.

Similar substitution chemistry is accomplished with the chelating ligand (pyrrolyl)$_2$P(CH$_2$)$_2$P(pyrrolyl)$_2$ (Scheme 2). Thus, addition of 1 equiv of this ligand to a THF solution of [PPN][Rh(CO)$_4$] results in CO evolution and disappearance (by IR) of starting material. In its place, a pair of bands at 1927 and 1877 cm^{-1} appear which are accompanied by the formation of a doublet in the ^{31}P NMR spectrum. These data are consistent with the formation of the dicarbonyl anion [PPN][Rh(CO)$_2$(pyrrolyl)$_2$P(CH$_2$)P(pyrrolyl)$_2$].

Scheme 2

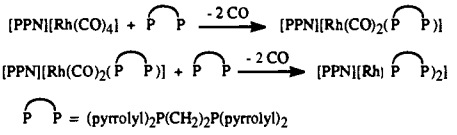

Addition of a second equivalent of the chelate (with heating and removal of evolved CO) results in complete displacement of CO ligands as determined by the complete loss of carbonyl bands in the IR spectrum. Again, both ^{31}P and ^{1}H NMR show essentially quantitative formation of a new complex with spectral properties consistent with an intact (pyrrolyl)$_2$P(CH$_2$)$_2$P(pyrrolyl)$_2$ ligand. Integration of ligand and PPN$^+$ resonances in both the ^{1}H and ^{31}P NMR spectra indicates that the ratio of coordinated ligand to PPN$^+$ in this new species is 2:1. These results and observations, together with the results obtained with P(pyrrolyl)$_3$, lead us to assign this new complex as the homoleptic anion [PPN][Rh{(pyrrolyl)$_2$P(CH$_2$)$_2$P(pyrrolyl)$_2$}$_2$]. Crystallization by slow diffusion of Et$_2$O into a THF solution of this anion allows the isolation of this complex in 36% yield as the THF monosolvate.

Infrared data for the new anionic complexes are summarized in Table 6, where they are compared to related complexes. The trend in the infrared spectra is the same as that observed in the Rh(I) series; a significant increase in ν_{CO} occurs with complexes of P(pyrrolyl)$_3$ relative to those of more traditional phosphorus ligands. For instance, in the series [Rh(CO)$_3$(PR$_3$)]$^-$, ν_{CO} for the P(pyrrolyl)$_3$ derivative is *ca.* 40 cm^{-1} higher in frequency than that found for PR$_3$ = PPh$_3$. P(pyrrolyl)$_3$ is again seen to be a weaker σ-donor and better π-acceptor than phosphites, where ν_{CO} occurs at higher frequency than that observed for analogous P(OPh)$_3$ complexes in all cases. A particularly dramatic example is seen in a comparison of the complexes [Rh(CO)(PR$_3$)$_3$]$^-$ where ν_{CO} is 120 cm^{-1} higher for PR$_3$ = P(pyrrolyl)$_3$ than that reported for PPh$_3$. These data further exemplify the π-acceptor properties of *N*-pyrrolyl phosphines.[39]

II. Molecular Structure of [PPN][Rh(CO){P(pyrrolyl)$_3$}$_3$]·C$_4$H$_8$O. A single crystal X-ray structure analysis of [PPN][Rh-

Table 6. Summary of Infrared and ^{31}P NMR Data for Rhodium Anion Complexes

complex	IR	^{31}P NMR δ (ppm)	^{31}P NMR $^{1}J_{P\text{-}Rh}$ (Hz)	ref
[PPN][Rh(CO)$_3$(P(pyrrolyl)$_3$)]	1970, 1900[a]	114.4	258	this work
[PPN][Rh(CO)$_2${P(pyrrolyl)$_3$}$_2$]	1943, 1897[a]	113.9	262	this work
[PPN][Rh(CO){P(pyrrolyl)$_3$}$_3$]	1919[a]	113.2	265	this work
[PPN][Rh{P(pyrrolyl)$_3$}$_4$]		111.3	266	this work
[PPN][Rh(CO)$_2${(pyrrolyl)$_2$P(CH$_2$)$_2$(pyrrolyl)$_2$}]	1927, 1874[a]	133.2	230	this work
[PPN][Rh{(pyrrolyl)$_2$P(CH$_2$)$_2$(pyrrolyl)$_2$}$_2$]		130.6	243	this work
[Bu$_4$N][Rh(CO)$_3$(PPh$_3$)]	1930, 1855[b]			36a
[Bu$_4$N][Rh(CO)$_2$(PPh$_3$)$_2$]	1855, 1805[b]			36a
[Bu$_4$N][Rh(CO)(PPh$_3$)$_3$]	1800[b]			36a
[K][Rh(CO)$_3${P(OPh)$_3$}]	1962, 1860[a]			35b
[K][Rh(CO)$_2${P(OPh)$_3$}$_2$]	1933, 1881[a]			35b
[Bu$_4$N][Rh(CO)$_2$(diphos)]	1860, 1805[b]			36b

[a] ^{31}P NMR data omit the PPN resonance at δ 21.9. NMR recorded in THF-d_8. [b] THF. [c] CH_3CN.

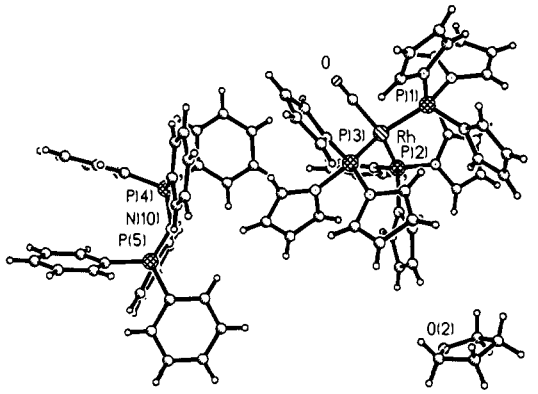

Figure 5. A partial view of the unit cell of [PPN][Rh(CO)-{P(pyrrolyl)$_3$}$_3$]·C$_4$H$_8$O showing the anion, PPN$^+$ counterion, and THF solvate.

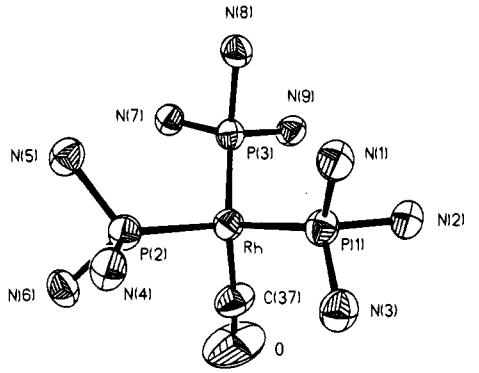

Figure 6. ORTEP drawing of the anion in [PPN][Rh(CO)-{P(pyrrolyl)$_3$}$_3$]·C$_4$H$_8$O. Ring carbons and hydrogens as well as the PPN$^+$ counterion and THF solvate have been omitted for clarity. Thermal ellipsoids are drawn at the 50% probability level.

(CO){P(pyrrolyl)$_3$}$_3$]·C$_4$H$_8$O was carried out and confirmed our structural assignment. A partial view of the unit cell showing the anion, PPN$^+$ counterion, and THF solvate is shown in Figure 5. Figure 6 provides a closer view of the anion, giving a better view of the coordination sphere about rhodium. Table 7 gives selected bond distances and angles.

The gross features of the structure are unremarkable. The rhodium(−1) ion is pseudotetradedral, as expected. In fact, an examination of Table 7 shows that the bond angles about rhodium are all within 2° of a perfect tetrahedral geometry. A slight deformation which folds the three P(pyrrolyl)$_3$ ligands toward the lone CO ligand is notable. This minor distortion indicates that steric constraints are minimal in this structure. This is of interest because the Rh−P distances average 2.205 Å, a value *ca.* 0.08 Å shorter than the average observed in RhCl-(CO)[P(pyrrolyl)$_3$]$_2$. This bond shortening indicates an increased degree of metal to ligand π-back-bonding in the anion, as would be anticipated in this electron rich system. Increased steric influences due to shortening of the Rh−P bond are at least partially compensated for by the flexibility of these ligands as determined by a consideration of the angles about phosphorus. For instance, the sum of N−P−N angles for each ligand averages 289°. This may be compared with the corresponding values found for the complex RhCl(CO)[P(pyrrolyl)$_3$]$_2$ of 306.5° (average value for molecules 1 and 2). This is accompanied by a slight increase in the average Rh−P−N angle in the anion (121°) versus that in the Rh(I) complex (116°). Thus, the P(pyrrolyl)$_3$ ligand found in the anion develops a slightly more "inverted umbrella" shape. The P−N bond lengths found in the anion are significantly longer (av 1.735 Å) than those found

Table 7. Selected Interatomic Distances (Å) and Bond Angles (deg) in [PPN][Rh(CO){P(NC$_4$H$_4$)$_3$}$_3$]·THF

A. Interatomic Distances

Rh−C(37)	1.894(6)	Rh−P(1)	2.209(2)
Rh−P(2)	2.195(2)	Rh−P(3)	2.212(2)
P(1)−N(1)	1.744(4)	P(1)−N(2)	1.727(5)
P(1)−N(3)	1.738(5)	P(2)−N(4)	1.738(4)
P(2)−N(5)	1.742(5)	P(2)−N(6)	1.736(5)
P(3)−N(7)	1.741(4)	P(3)−N(9)	1.735(4)
P(3)−N(9)	1.737(4)	O−C(37)	1.136(6)

B. Ring Bond Lengths

	N−C$_\alpha$	C$_\alpha$−C$_\beta$	C$_\beta$−C$_\beta$
range	1.355−1.387	1.340−1.361	1.376−1.411
average	1.373	1.349	1.394

C. Bond Angles

C(37)−Rh−P(1)	108.1(2)	C(37)−Rh−P(2)	107.6(2)
C(37)−Rh−P(3)	108.1(2)	P(1)−Rh−P(2)	110.81(6)
P(1)−Rh−P(3)	111.67(6)	P(2)−Rh−P(3)	110.46(6)
N(1)−P(1)−N(2)	96.0(2)	N(1)−P(1)−N(3)	96.7(2)
N(2)−P(1)−N(3)	97.2(2)	N(1)−P(1)−Rh	121.2(2)
N(2)−P(1)−Rh	121.9(2)	N(3)−P(1)−Rh	118.2(2)
N(4)−P(2)−N(5)	96.2(2)	N(4)−P(2)−N(6)	95.6(2)
N(5)−P(2)−N(6)	96.9(2)	N(4)−P(2)−Rh	123.5(2)
N(5)−P(2)−Rh	121.7(2)	N(6)−P(2)−Rh	116.8(2)
N(7)−P(3)−N(8)	95.7(2)	N(7)−P(3)−N(9)	95.9(2)
N(8)−P(3)−N(9)	97.0(2)	N(7)−P(3)−Rh	122.3(2)
N(8)−P(3)−Rh	122.0(2)	N(9)−P(3)−Rh	118.0(2)

(39) [PPN][Rh(CO)$_3${P(C$_6$H$_{11}$)$_3$}] has also been reported.[10a] However, this assignment does not appear to be reasonable. Only a single IR band (ν_{CO} = 1841 cm^{-1}) is reported for this complex, and it was generated in the presence of CO, where it would be expected to be rapidly converted to [Rh(CO)$_4$]$^-$.

Table 8. Crystallographic Data for the X-ray Diffraction Analyses of Rh(CO)Cl[P(pyrrolyl)$_3$]$_2$, Rh(CO)Cl[P(pyrrolidinyl)$_3$]$_2$, and [PPN][Rh(CO){P(pyrrolyl)$_3$}$_3$]·THF

	A. Crystal Data		
empirical formula	$C_{25}H_{24}RhClOP_2N_6$	$C_{25}H_{48}RhClOP_2N_6$	$C_{77}H_{74}RhO_2P_5N_{10}$
color	yellow	yellow	yellow
crystal dimensions, mm	0.12 × 0.22 × 0.24	0.12 × 0.12 × 0.07	0.24 × 0.38 × 0.50
temperature, K	295(2)	173(2)	295(2)
crystal system	monoclinic	triclinic	triclinic
space group	$P2_1/c$ (C_{2h}^5, no. 14)	$P\bar{1}$ (C_i^1, no. 2)	$P\bar{1}$ (C_i^1, no. 2)
a, Å	24.205(3)	9.512(1)	13.649(3)
b, Å	14.170(2)	11.967(2)	13.817(5)
c, Å	16.924(2)	13.999(2)	19.655(6)
α, deg		86.33(1)	77.65(2)
β, deg	110.375(8)	71.48(1)	88.02(2)
γ, deg		75.27(1)	88.15(2)
vol, Å^3	5441.7(11)	1461.1(4)	3618(2)
Z	8	2	2
formula wt, amu	624.8	649.0	1429.22
calcd density, g/cm^3	1.525	1.475	1.312
μ, cm^{-1}	8.73	8.15	4.00
$F(0\,0\,0)$	2528	680	1484
	B. Data Collection and Structural Analyses		
scan type	ω, variable	ω, variable	ω, variable
scan rate, deg/min	2.50−5.00	2.00−10.00	4.00−10.00
2θ range, deg	3.0−50.0	2.0−50.0	3.0−50.0
index ranges	$-28 \le h \le 28$	$0 \le h \le 10$	$0 \le h \le 16$)
	$0 \le k \le 16$	$-13 \le k \le 14$	$-16 \le k \le 16$)
	$0 \le l \le 20$	$-15 \le l \le 16$	$-23 \le l \le 23$)
no. of refl. collected	9779	5455	13176
agreement between equiv data, $R_{av}(F_o)$	0.023	0.014	0.0411
total no. of unique data	9539	5056	12593
obsd data criteria	$F_o > 4.0\,\sigma(F_o)$	$F_o > 4.0\,\sigma(F_o)$	$F_o > 4.0\,\sigma(F_o)$
no. of obsd data	4556	4283	7150
absorption correction	face-indexed	none	empirical (PSI scans)
range of trans. coefficients	0.823−0.901		0.87−0.92
p	0.0010	0.0008	
refinement method	full-matrix on F	full-matrix on F	full-matrix on $F2$
discrepancy indices			
$R(F_o)$	0.0644	0.0328	0.0617
$R_w(F_o)$	0.0769	0.0443	0.1030
GOF	1.35	1.03	1.01
no. of variables	649	325	902
data to parameter ratio	7.0:1	13.2:1	12.1:1

in RhCl(CO)[P(pyrrolyl)$_3$]$_2$ (av 1.690 Å). This is consistent with previous observations which demonstrate that, as metal to phosphorus back-bonding increases in M−PZ$_3$ complexes, the P−Z bond length also increases.[1f] This has been used as evidence for back-bonding into P−Z σ^* orbitals instead of phosphorus d orbitals in complexes of phosphorus(III) ligands.

A comparison of the [PPN][Rh(CO){P(pyrrolyl)$_3$}$_3$] structure with those determined by Chan[34b] for [Rh(CO)$_3$(PPh$_3$)]$^-$, [Rh(CO)$_2${Ph$_2$P(CH$_2$)$_2$PPh$_2$}]$^-$, and [Rh(CO)$_2${P(OPh)$_3$}$_2$]$^-$ is confounded by significant ion pairing with the alkali metal (Na$^+$, K$^+$) counterions. In the PPh$_3$ and Ph$_2$P(CH$_2$)$_2$PPh$_2$ structures one oxygen of a carbonyl ligand is coordinated to a sodium cation. In the P(OPh)$_3$ structure a potassium cation is coordinated to a phosphite oxygen atom. One trend can be seen, however. Phosphorus ligands which are good σ-donors and relatively poor π-acceptors result in long Rh−P bond lengths in these anions. Thus, Rh−P in [Rh(CO)$_3$(PPh$_3$)]$^-$ is 2.32 Å, and that in [Rh(CO)$_2${Ph$_2$P(CH$_2$)$_2$PPh$_2$}]$^-$ is 2.30 Å. As expected, ligands with enhanced π-acceptor character possess significantly shorter Rh−P bond lengths: 2.205 Å for the P(pyrrolyl)$_3$ structure reported here and 2.212 Å for non-ion paired phosphite ligand in [Rh(CO)$_2${P(OPh)$_3$}$_2$]$^-$.

Competitive Ligand Exchange in Anionic Rh(−I) Complexes: P(pyrrolyl)$_3$ *vs* PPh$_3$. The results presented thus far indicate that Rh(−I) prefers ligands with π-acceptor character. This is, of course, exactly the opposite trend observed for Rh(I), as demonstrated by the results of ligand exchange reaction shown in eq 5. In an effort to quantify these observations we attempted to determine the equilibrium constant for the reaction shown in eq 8. To do this we attempted to measure the individual equilibrium constants for the reactions shown in eqs 6 and 7, and from those derive that for eq 8.

$$[Rh(CO)_3PPh_3]^- + CO \rightleftharpoons [Rh(CO)_4]^- + PPh_3 \quad (6)$$

$$[Rh(CO)_4]^- + P(pyrrolyl)_3 \rightleftharpoons [Rh(CO)_3P(pyrrolyl)_3]^- + CO \quad (7)$$

$$[Rh(CO)_3PPh_3]^- + P(pyrrolyl)_3 \rightleftharpoons [Rh(CO)_3P(pyrrolyl)_3]^- + PPh_3 \quad (8)$$

However, we find that the equilibrium shown in eq 7 lies very far to the right, even at high partial pressures of CO. For instance, we detect no conversion of [Rh(CO)$_3${P(pyrrolyl)$_3$}]$^-$ to [Rh(CO)$_4$]$^-$ at 115 psia CO. The tenacity of P(pyrrolyl)$_3$ to coordinate to this electron rich metal center is further exemplified by the failure to displace P(pyrrolyl)$_3$ from [Rh(CO)$_2$-{P(pyrrolyl)$_3$}$_2$]$^-$, also at 115 psia CO. Only with the monocarbonyl [Rh(CO){P(pyrrolyl)$_3$}$_3$]$^-$ is P(pyrrolyl)$_3$ displacement observed at these CO partial pressures (eq 9), and then only *ca.* 30% conversion to the dicarbonyl occurs.

$$[Rh(CO)\{P(pyrrolyl)_3\}_3]^- + CO \rightleftharpoons [Rh(CO)_2\{P(pyrrolyl)_3\}_2]^- + P(pyrrolyl)_3 \quad (9)$$

$$K_{eq} = 0.19 \pm 0.05 \quad (25\ °C)$$

These results may be contrasted with those reported for PPh_3 by Chan *et al.*,[35] as discussed above. Consistent with those reports, we find that $[Rh(CO)_3PPh_3]^-$ is completely converted to $[Rh(CO)_4]^-$ and free PPh_3 with 75 psia CO. Although a quantitative measurement of the equilibrium constant for eq 8 has not yet been determined, a lower limit of $K \geq 3000$ can be estimated from the available data.[40]

Conclusions

N-Pyrrolyl phosphines have been shown to be a novel class of ligands possessing exceptional π-acceptor properties. Although the unusual reactivity of these compounds had been recognized previously, their utility in coordination chemistry was not. The π-acceptor ability of *N*-pyrrolyl phosphines are not quite equal to those of the fluoroalkyl phosphine ligands recently reported, but do rival those of $P(C_6F_5)_3$, and exceed those of phosphites such as $P(OPh)_3$. It should be pointed out, however, that the present work only describes the parent compounds in this general class. A tremendous variety of similar substituents such as substituted pyrroles, indoles, imidazoles, pyrazoles, etc., are commercially available or obtainable by synthetic means. Thus, it should be possible to prepare *N*-pyrrolyl-like phosphines which possess electronic properties comparable to fluoroalkyl phosphines and, perhaps, halophosphines such as PCl_3 and PF_3. The simple synthesis of these ligands, together with the wide variety of accessible pyrrole-like precursors make it an attractive area of study with potentially greater promise than fluoroalkyl phosphine ligand chemistry.[41]

From the X-ray investigations reported herein, it is concluded that *N*-pyrrolyl, phenyl, and *N*-pyrrolidinyl substituents make essentially equal contributions to ligand cone angles. Thus, it is interesting to consider the potential utility of the isosteric series of ligands shown below (pyrl = pyrrolyl; pyrldn = pyrrolidinyl). This series spans nearly the entire range of phosphine electronic properties, ranging from the extremes of an excellent π-acceptor ($P(pyrrolyl)_3$) to a potent σ-donor ($P(pyrrolidinyl)_3$) equal in basicity to tris(alkyl) phosphines such as P^nBu_3. Note that within this series, ν_{CO} varies by 72 cm^{-1} for the complexes *trans*-$RhCl(CO)(PZ_3)_2$ (Table 2). Moreover, as shown by the data in Figure 1, it is relatively simple to adjust these properties in a methodical manner. An understanding of the influence of phosphine structure on the chemical properties of metal complexes is often confounded by contributions from both steric and electronic factors. As a result, attempts to delineate these contributions often rely on the investigation of ligands with equal cone angles (e.g., isosteric) but variable electronic properties, such as para-substituted derivatives of triphenyl phosphine ($P(p\text{-}XC_6H_4)_3$). The series of phosphine ligands described here covers a far greater range of σ-donor/π-acceptor properties and is more readily accessible than any other isosteric series known. As a result, we propose that consideration be given to the use of these ligands in physical inorganic and organometallic studies of ligand-influenced metal reactivity.

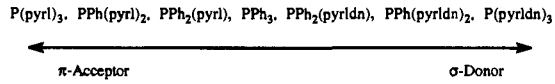

Experimental Section

General Considerations. All manipulations were carried out under inert atmosphere using a glovebox, Schlenk line, or high pressure manifold. THF and Et_2O were distilled from NaK/benzophenone. Toluene and hexane were purchased from Aldrich as anhydrous grade material and used as received. Deuterated solvents were dried over the appropriate agents and vacuum transferred. [PPN][$Rh(CO)_4$] was prepared by the literature method.[42] Pyrrole, pyrrolidine, and Et_3N were distilled from Na and stored under nitrogen. PCl_3, $PhPCl_2$, Ph_2PCl, and $Cl_2PCH_2CH_2PCl_2$ were obtained from commercial vendors and used as received.

Proton, phosphorus, and carbon NMR data were collected in the Union Carbide Corp. NMR Skill Center using General Electric GN-300NB and QE-300 spectrometers (each are 300 MHz ^1H). The ^1H and ^{13}C spectra were normally referenced to TMS *via* solvent peaks, and the ^{31}P spectra were referenced externally to 85% phosphoric acid. Infrared spectra were recorded on a Nicolet 205 FTIR spectrometer as solutions or Nujol mulls with CaF_2 cells or plates. Elemental analyses were performed by Galbraith Analytical Laboratories, Knoxville, TN, or by Desert Analytics, Tucson, AZ.

P(pyrrolyl)$_3$. A flame dried Schlenk flask was placed under inert atmosphere and then charged with 32.0 mL (30.9 g, 0.461 mol) of pyrrole, 70 mL (51 g, 0.50 mol) of Et_3N, and 200 mL of THF. The solution was cooled to −78 °C, and 10.0 mL (15.7 g, 0.115 mol) of PCl_3 was added by syringe. A colorless precipitate formed immediately. After 10 min the mixture was allowed to warm to ambient temperature. After 30 min at ambient temperature the flask was immersed in a 65 °C oil bath such that the liquid and oil levels were coincident. After 24 h a thick suspension of colorless solid was obtained, and ^{31}P NMR showed nearly complete conversion to the desired product (a trace amount of $ClP(pyrrolyl)_2$ was observed at δ 103). The solids were removed by filtration and washed with two 50 mL portions of THF. The filtrates were combined and taken to dryness under vacuum to yield a crystalline off-white mass. The product was dissolved in 100 mL of hexane, and a small amount of insoluble material was removed by filtration. The solution was concentrated *in vacuo* to *ca.* 40 mL and then slowly cooled to −78 °C to precipitate the product as colorless crystals. These were isolated by filtration and dried under vacuum: yield 19.4 g, 74%. $^{31}P\{^1H\}$ NMR (toluene-d_8) δ 79.6; ^1H (toluene-d_8) 6.55 (overlapping doublet of pseudo triplets, 6 H), 6.21 (pseudo-triplet, 6 H).

(pyrrolyl)$_2$P(CH$_2$)$_2$P(pyrrolyl)$_2$. A Schlenk flask was charged with 9.1 mL (8.8 g, 0.13 mol) of pyrrole, 18.2 mL (13.2 g, 0.13 mol) of Et_3N and 130 mL of toluene. To the resulting solution was added via an addition funnel, at room temperature, a solution of 5.99 g (0.0259 mol) of $Cl_2P(CH_2)_2PCl_2$ in 30 mL of toluene. A light yellow color and a precipitate formed immediately, and heat was evolved. The addition was done slowly and with good stirring to keep the reaction temperature below 40 °C. After the addition was complete the mixture was stirred for 3 days at room temperature, after which time ^{31}P NMR analysis indicated complete reaction. The solids were removed by filtration and washed with two portions of toluene. The solvent was removed under vacuum and the crude product was dried thoroughly under high vacuum: yield 8.35 g, 91%. This material (7.30 g) was recrystallized from warm toluene (ca. 75 mL). The crystals were washed with hexane and dried under vacuum to give 5.50 g of pure product: $^{31}P\{^1H\}$ NMR ($CDCl_3$) δ 68.4; ^1H (CD_2Cl_2) 6.98 (overlapping doublet of pseudo triplets, 8 H), 6.30 (pseudo-triplet, 4 H), 2.34 (t, 4H).

(40) This lower limit is estimated by assuming that the phosphine displacement in eq 6 occurs to the extent of 95% (estimated ^{31}P NMR detection limit) at 75 psia CO, and that CO displacement by $P(pyrrolyl)_3$ in eq 7 occurs to the extent of 95% at 115 psia CO. From these assumptions, equilibrium constants of *ca.* 12 and 210 can be calculated for eqs 6 and 7, respectively (see Experimental Section for further details). Thus, it follows that for eq 8, $K \geq 3000$.

(41) We have recently prepared P(*N*-indolyl)$_3$ and find that this ligand, as expected, possesses electronic properties similar to $P(pyrrolyl)_3$. This is demonstrated by the infrared spectrum of *trans*-$RhCl(CO)[P(indolyl)_3]_2$ which shows ν_{CO} = 2019 cm^{-1}.

(42) Garlaschelli, L.; Della Perzola, R.; Martinengo, S. *Inorg. Synth.* **1990**, *28*, 211.

PhP(pyrrolyl)$_2$. A 500 mL Schlenk flask was charged with 120 mL of THF, 21 mL (0.30 mol) of pyrrole, and 42 mL (0.30 mol) of Et_3N. The solution was cooled to 0 °C and 8.4 mL (0.062 mol) of $PhPCl_2$ was added dropwise. A colorless precipitate formed immediately. When the addition was complete, the suspension was warmed to room temperature and stirred for 1 h, followed by 1 h at 65 °C. At this time ^{31}P NMR showed complete conversion to the desired product. The suspension was filtered, and the solvent was removed *in vacuo*. The crude oily product was redissolved in toluene and again filtered to remove residual Et_3NHCl. The toluene was removed under vacuum to again yield an oil. The product was crystallized from hexane as colorless crystals: yield 12.4 g, 82%; $^{31}P\{^1H\}$ NMR (toluene-d_8) δ 70.6; ^1H NMR (toluene-d_8) δ 7.05−6.85 (m, 5 H); 6.80 (overlapping doublet of pseudo-triplets, 4 H); 6.26 (pseudo-triplet, 4 H).

Ph$_2$P(pyrrolyl). Ph_2PCl (10.12 g, 0.0459 mol), 29 mL of Et_3N (0.20 mol), and 50 mL of THF were charged to a Schlenk flask. This was followed by 14 mL (0.20 mol) of pyrrole. The solution was refluxed for 15 h. The colorless precipitate which formed was removed by filtration and washed with THF. The combined filtrates were taken to dryness under vacuum. The resulting oil was redissolved in hexane and filtered. The solvent was removed under vacuum to give the product as an oil (lit.: bp = 100 °C at 1 Torr): yield 9.3 g, 80%; $^{31}P\{^1H\}$ NMR (THF) δ 48.1.

P(pyrrolidinyl)$_3$. A 100 mL Schlenk flask was charged with 1.60 mL (2.52 g, 0.0183 mol) of PCl_3 and 20 mL of THF. The solution was cooled in an ice bath and a solution of 10.0 mL (8.52 g, 0.120 mol) of pyrrolidine (dried over Na) in 10 mL of THF was added dropwise, with stirring. A colorless precipitate formed immediately, and heat was generated. When the addition was complete the suspension was warmed to room temperature and stirring was continued. The reaction was halted when ^{31}P NMR analysis showed complete conversion to the desired product (generally overnight). The mixture was filtered, and the solids were washed with THF. The solvent was removed under vacuum to yield a colorless oil and some colorless solids. The oil was dissolved in toluene and filtered, and the solvent again was removed under vacuum. The resulting product may be used as obtained or distilled (lit.:[6] 104°, 0.1 Torr) before use: ^1H NMR ($CDCl_3$) δ 2.9−2.5 (m, 4H), 1.5−1.1 (m, 4H); $^{31}P\{^1H\}$ NMR ($CDCl_3$) δ 104.9.

General Method for Generation and Infrared Characterization of RhCl(CO)P$_2$. A solution of 0.10 g (0.51 mmol) of $[RhCl(CO)_2]_2$ in 5 mL of CH_2Cl_2 was prepared in the glovebox. To this was then added 1.29 mmol (2.5 equiv) of the phosphine ligand. Gas evolution generally occurred immediately and was accompanied by a color change from red-orange to bright yellow. After ca. 15 min an aliquot was withdrawn for IR analysis which in all cases showed quantitative conversion to *trans*-$RhCl(CO)P_2$. ^{31}P NMR of these solutions was found not to be useful due to rapid exchange, resulting in broadened peaks with chemical shifts intermediate between those of free and the excess coordinated ligand. Infrared data are provided in Table 2. In a few cases the complexes were purified of excess ligand and analyzed in greater detail, as described below.

Preparation of *trans*-RhCl(CO)[P(pyrrolyl)$_3$]$_2$. $[Rh(CO)_2Cl]_2$ (0.308 g, 1.59 mmol Rh) was dissolved in 14 mL of CH_2Cl_2 to give a red solution. P(pyrrolyl)$_3$ (0.78 g, 3.40 mmol) was added portion-wise resulting in immediate gas evolution and a change in color to bright yellow. After 2 h the solvent was concentrated, and yellow crystals formed. Hexane was added, resulting in the formation of more precipitate. The solids were dissolved by gentle heating, and the saturated solution was allowed to slowly cool over a 2 day period to −78 °C. The bright yellow crystals were isolated by filtration and dried under vacuum: yield 0.894 g, 91%; $^{31}P\{^1H\}$ (CD_2Cl_2) δ 89.2 (d, J_{Rh-P} = 179.7 Hz); ^1H (CD_2Cl_2) δ 7.08 (m, 2H), 6.46 (m, 2H); IR (CH_2Cl_2) 2024 cm^{-1}. Elemental Anal. Calcd for $C_{25}H_{24}ClN_6OP_2Rh$: C, 48.06; H, 3.87; N, 13.45; P, 9.91. Found: C, 48.08; H, 3.84; N, 13.41; P, 10.31.

Preparation of *trans*-RhCl(CO)[PPh$_2$(pyrrolyl)]$_2$. This complex was prepared in a similar fashion as that described for *trans*-RhCl(CO)[P(pyrrolyl)$_3$]$_2$, above: $^{31}P\{^1H\}$ (CD_2Cl_2) δ 71.7 (d, J_{Rh-P} = 140 Hz); ^1H (CD_2Cl_2) δ 7.65−7.40 (m, 10H), 6.36 br s, 2H), 6.36 (m, 2H).

Preparation of *trans*-RhCl(CO)[P(pyrrolidinyl)$_3$]$_2$. This complex was prepared in a similar manner using 0.358 g (1.84 mmol Rh) of $[Rh(CO)_2Cl]_2$, 1.00 g (4.14 mmol) of P(pyrrolidinyl)$_3$, and 20 mL of CH_2Cl_2. The yellow crystalline product was isolated by removing the solvent under vacuum and washing twice with hexane: yield 1.17 g, 98%; $^{31}P\{^1H\}$ (tol-d_8) δ 98.5 (d, J_{Rh-P} = 146 Hz); ^1H (tol-d_8) δ 3.40 (m, 4H), 1.70 (m, 4H); IR (CH_2Cl_2, cm^{-1}) 1952. Elemental Anal. Calcd for $C_{25}H_{48}ClN_6OP_2Rh$: C, 46.27; H, 7.45; N, 12.95; P, 9.55. Found: C, 46.76; H, 7.48; N, 13.33; P, 9.85.

[RhCl[(pyrrolyl)$_2$P(CH$_2$)$_2$P(pyrrolyl)$_2$]]$_x$. This complex was prepared similarly with 0.276 g (1.42 mmol Rh) of $[Rh(CO)_2Cl]_2$, 0.526 g (1.48 mmol) of $(pyrrolyl)_2P(CH_2)_2P(pyrrolyl)_2$, and 12 mL of CH_2Cl_2. The crude product was isolated by removing the solvent under vacuum. Crystals were obtained by slowly cooling a hot, saturated toluene solution: yield 0.582 g; $^{31}P\{^1H\}$ ($CDCl_3$) δ 125.1 (d, J_{Rh-P} = 240.2 Hz); ^1H ($CDCl_3$) 7.20 (m, 8H), 6.31 (m, 8H), 2.27 (pseudo-doublet, 4H). The ^1H spectrum also showed significant amounts of toluene. Elemental Anal. Calcd for $C_{18}H_{20}ClN_4P_2Rh{\cdot}0.3(C_7H_8)$: C, 46.40; H, 4.34; N, 10.77; P, 11.91. Found: C, 46.53; H, 4.33; N, 10.42; P, 9.99.

Mo(CO)$_4$[(pyrrolyl)$_2$P(CH$_2$)$_2$P(pyrrolyl)$_2$]. $(pyrrolyl)_2P(CH_2)_2$-P(pyrrolyl)$_2$ (1.00 g, 2.82 mmol) , 0.74 g (2.82 mmol) of $Mo(CO)_6$, and 15 mL of toluene were combined in a Schlenk flask fitted with a reflux condenser. The mixture was brought to a gentle reflux. After 21 h infrared analysis showed no $Mo(CO)_6$ remained. The solvent was removed under vacuum, and the beige product redissolved in THF. Hexane was added to precipitate the beige product which was isolated by filtration and dried under vacuum: yield: 1.16 g, 73%. The product was recrystallized by dissolving in hot toluene and filtering off an insoluble brown residue. Upon slow cooling to room temperature colorless crystals formed: $^{31}P\{^1H\}$ NMR (toluene-d_8) δ 135.7; ^1H (toluene-d_8) δ 6.81 (pseudo-quintet, 8H), 6.13 (pseudo-triplet, 8H), 2.08 (pseudo-doublet, 4H); IR (Nujol, cm^{-1}) 2043, 1968, 1960, 1944, 1904; IR (toluene, cm^{-1}) 2044, 1970, 1916. Elemental Anal. Calcd for $C_{22}H_{20}N_4O_4P_2Mo$: C, 46.99; H, 3.58; N, 9.96; P, 11.02. Found: C, 46.56; H, 3.58; N, 9.56; P, 11.07.

Ligand Exchange in *trans*-RhCl(CO)[P(NR$_2$)$_3$]$_2$. P(pyrrolyl)$_3$ *vs* P(pyrrolidinyl)$_3$. $RhCl(CO)[P(pyrrolyl)_3]_2$ (0.0316 g, 0.0506 mmol) was dissolved in 3.0 mL of CH_2Cl_2. An aliquot was removed and analyzed by IR which showed the expected band at 2024 cm^{-1}. Next, 0.0159 g (0.0659 mmol, 1.3 equiv) of P(pyrrolidinyl)$_3$ was added. After 1.5 h at ambient temperature an aliquot was removed for IR analysis which showed the complete disappearance of $RhCl(CO)[P(pyrrolyl)_3]_2$ and the formation of two new bands at 1988 and 1952 cm^{-1}. The latter band is attributable to $RhCl(CO)[P(pyrrolidinyl)_3]_2$. Another 0.0146 g (0.0605 mmol) of P(pyrrolidinyl)$_3$ was added. This resulted in loss of the 1988 cm^{-1} band and quantitative conversion to $RhCl(CO)[P(pyrrolidinyl)_3]_2$.

In a separate experiment, 0.0355 g (0.0547 mmol) of $RhCl(CO)[P(pyrrolidinyl)_3]_2$ was dissolved in 3.0 mL of CH_2Cl_2. An aliquot was removed and analyzed by IR which showed the expected band at 1952 cm^{-1}. P(pyrrolyl)$_3$ (0.0182 g, 0.0793 mmol, 1.45 equiv) was then added, and the solution was monitored by IR. No reaction was noted after several hours at ambient temperature.

Titration of [PPN][Rh(CO)$_4$] with P(pyrrolyl)$_3$. [PPN][$Rh(CO)_4$] (0.10 g, 0.13 mmol) was dissolved in 4 mL of THF. P(pyrrolyl)$_3$ (1 equiv, 0.030 g) was then added, and gas evolution occurred immediately. After stirring for several hours at room temperature, two new carbonyl species were observed by IR and ^{31}P NMR spectroscopies. The major component (*ca.* 90%) is assigned to [PPN][$Rh(CO)_3${P(pyrrolyl)$_3$}], and the minor component is assigned to [PPN][$Rh(CO)_2${P(pyrrolyl)$_3$}$_2$] (see Table 6 for IR and ^{31}P NMR data). An additional equivalent of P(pyrrolyl)$_3$ was added to the solution, and the procedure was repeated. Spectroscopic analysis showed complete conversion to [PPN][$Rh(CO)_2${P(pyrrolyl)$_3$}$_2$]. An additional 3 equiv of P(pyrrolyl)$_3$ were added (5 equiv total). After stirring the mixture for several hours the solution was again analyzed by ^{31}P NMR and IR spectroscopies. These data showed the disappearance of the dicarbonyl and formation of a new species identified as [PPN][$Rh(CO)${P(pyrrolyl)$_3$}$_3$]. Finally, heating the resulting solution at 65 °C resulted in a very slow conversion to a new species devoid of a carbonyl ligand (IR) and assigned to [PPN][Rh{P(pyrrolyl)$_3$}$_4$].

Preparation of [PPN][Rh(CO){P(pyrrolyl)$_3$}$_3$]. [PPN][$Rh(CO)_4$] (0.297 g, 0.394 mmol) and 0.472 g (2.06 mmol) P(pyrrolyl)$_3$ were combined in 20 mL of THF. Gas evolution was immediate, and the solution turned a straw yellow color. The solution was allowed to stand

at room temperature, and the vessel was periodically evacuated to remove evolved CO. After 14 h, IR showed a single strong band at 1919 cm^{-1}, attributable to the desired complex. Solvent was removed under vacuum to yield an oily, gummy product. The product was triturated with two 5 mL portions of Et_2O to yield a cream colored powder. This was dissolved in 3 mL of THF and 10 mL of Et_2O was carefully layered on top of the solution. After standing overnight crystals had precipitated. The solution was cooled to 0 °C for 2 h, and then the crystals were harvested by filtration and dried under vacuum: yield 0.465 g, 83% calculated as the THF solvate [PPN][Rh(CO){P(pyrrolyl)$_3$}$_3$]·C_4H_8O; ^{1}H NMR (THF-d_8) δ 7.70−7.40 (m, 30 H); 6.28 (br s, 18H); 5.85 (m, 18H). Resonances resulting from THF of solvation are observed at δ 3.62 and 1.78. ^{31}P NMR parameters are provided in Table 6; careful integration of the coordinated P(pyrrolyl)$_3$ and PPN^+ ^{31}P NMR resonances gave the correct 3:2 ratio.

Preparation of [PPN][Rh{P(pyrrolyl)$_3$}$_4$]. [PPN][Rh(CO)$_4$] (0.247 g, 0.328 mmol) and 0.705 g (3.08 mmol) P(pyrrolyl)$_3$ were dissolved in 15 mL of THF. Gas evolution was immediate, and the solution turned a straw yellow. Gross amounts of evolved CO were removed by vacuum, and the solution was placed under 1 atm of N_2. The vessel was then immersed in a 85 °C oil bath. The vessel was periodically removed from the bath, and the contents were evacuated to remove evolved CO and replaced with fresh nitrogen. IR monitoring showed ca. 90% conversion after 55 h. After 96 h IR and ^{31}P NMR showed complete conversion to product. The solvent was removed under vacuum to yield an oil which gradually solidified. After trituration with Et_2O (two 6 mL portions) a cream colored powder was obtained. The product was redissolved in 3 mL of THF, and 15 mL of Et_2O was carefully layered on top of the solution. Upon standing overnight at room temperature a crystalline product was obtained. After cooling at 0 °C for 3 h the product was collected by filtration and dried under vacuum: yield 0.454 g, 85% calculated as the THF solvate [PPN][Rh{P(pyrrolyl)$_3$}$_4$]·C_4H_8O. ^{1}H NMR (THF-d_8) δ 7.72−7.44 (m, 30 H); 5.94 (br s, 24H); 5.78 (m, 24H). Resonances due to THF of solvation are observed at δ 3.62 and 1.78. Careful integration of the coordinated P(pyrrolyl)$_3$ and PPN^+ ^{31}P resonances (^{31}P NMR parameters are provided in Table 6) gave the correct 2:1 ratio. Elemental Anal. Calcd for $C_{84}H_{78}N_{13}P_6Rh$·C_4H_8O: C, 64.83; H, 5.32; N, 11.17; P, 11.40. Found: C, 65.10; H, 5.40; N, 11.15; P, 11.07.

Reaction of [PPN][Rh(CO)$_4$] with (pyrrolyl)$_2$P(CH$_2$)$_2$P(pyrrolyl)$_2$. I. *In situ* characterization of [[PPN][Rh(CO)$_2${(pyrrolyl)$_2$P(CH$_2$)$_2$-P(pyrrolyl)$_2$}] and [PPN][Rh{(pyrrolyl)$_2$P(CH$_2$)$_2$P(pyrrolyl)$_2$}$_2$]. [PPN][Rh(CO)$_4$] (0.0510 g, 0.0677 mol) was dissolved in 3 mL of THF. Then 0.0203 g (0.0573 mmol) of (pyrrolyl)$_2$P(CH$_2$)$_2$P(pyrrolyl)$_2$ was added. Slow gas evolution was visually apparent, and the solution turned straw yellow. The reaction was monitored by infrared spectroscopy, which showed complete conversion of $[Rh(CO)_4]^-$ to $[Rh(CO)_2$(pyrrolyl)$_2$P(CH$_2$)$_2$P(pyrrolyl)$_2]^-$ after 5 h at room temperature. This latter complex was identified by the presence of two carbonyl bands in the infrared spectrum at 1927 and 1877 cm^{-1}. ^{31}P NMR showed a doublet at δ 133.8 and J_{Rh-P} = 225 Hz. An additional 0.0365 g (0.103 mmol) of (pyrrolyl)$_2$P(CH$_2$)$_2$P(pyrrolyl)$_2$ was added to the solution, which was then transferred to a Carius tube. After freeze−pump−thaw degassing the solution, the tube was sealed *in vacuo* and immersed in a 65 °C oil bath. After 2.5 h the solution was cooled and analyzed. Infrared spectroscopy showed complete loss of carbonyl bands. ^{31}P NMR showed, in addition to resonances attributable to PPN^+ and excess ligand, a new doublet at δ 130.9 (J_{Rh-P} = 244 Hz) assigned to $[Rh${(pyrrolyl)$_2$P(CH$_2$)$_2$P(pyrrolyl)$_2$}$_2]^-$.

II. Preparation of [PPN][Rh{(pyrrolyl)$_2$P(CH$_2$)$_2$P(pyrrolyl)$_2$}$_2$]. On a preparative scale, 0.182 g (0.242 mmol) of [PPN][Rh(CO)$_4$)] and 0.210 g (0.593 mmol) of (pyrrolyl)$_2$P(CH$_2$)$_2$P(pyrrolyl)$_2$ were combined in a Carius tube. THF (6 mL) was added, giving a red solution and immediate gas evolution. The color faded within minutes to give a straw yellow solution which continued to slowly effervesce. The solution was degassed in vacuo, and the tube was immersed in a 65 °C oil bath, under vacuum. After 1 h the solution was again degassed and then heated for an additional 1 h. The solvent was removed under vacuum and the tacky foam was washed with two 5 mL portions of Et_2O. The resulting powder was then redissolved in ca. 3 mL of THF, and Et_2O was added by slow diffusion. This resulted in the formation of yellow crystals of the desired complex: yield 0.125 g, 36% (0.0879 mmol) based on one THF molecule of solvation, [PPN][Rh{(pyrrolyl)$_2$-P(CH$_2$)$_2$P(pyrrolyl)$_2$}$_2$]·C_4H_8O; ^{1}H NMR (THF-d_8) δ 7.65−7.40 (m, 30 H); 6.89 (br s, 16H); 5.79 (m, 16H), 2.29 (m, 8H). Resonances due to THF of solvation are observed at δ 3.62 and 1.78. Careful integration of the coordinated P(pyrrolyl)$_3$ and PPN^+ ^{31}P resonances gave the correct 2:1 ratio. Elemental Anal. Calcd for $C_{72}H_{70}N_9P_6Rh$·C_4H_8O: C, 64.18; H, 5.53; N, 8.86; P, 13.07. Found: C, 63.71; H, 5.34; N, 8.73; P, 11.96.

^{31}P NMR Study of Anionic Rhodium-Phosphine Complexes under CO. I. P(pyrrolyl)$_3$. [PPN][Rh(CO)$_4$] (0.0363 g, 0.0482 mmol) and 0.0148 g (0.0646 mmol) of P(pyrrolyl)$_3$ were dissolved in 0.6 mL of THF; gas evolution was noted. A portion of the solution was transferred to a high pressure, heavy walled 5 mm NMR tube (Wilmad Pressure Valve NMR Tube, Cat. No. 522-PV). After several hours at 25 °C, ^{31}P NMR showed the presence of a mixture of the anions $[Rh(CO)_3$P(pyrrolyl)$_3]^-$ and $[Rh(CO)_2${P(pyrrolyl)$_3$}$_2]^-$ (*ca.* 3:1 ratio, respectively). The tube was then connected to a high pressure manifold with an 1/8″ Teflon ferrule-nut (Alltech Associates, Stock No. 45701). The tube was pressurized/vented numerous times with CO and finally pressurized to 115 psia. The solution was agitated to ensure good mixing between the solution and gas phase. After standing overnight at 25 °C the tube was again subjected to the pressure/vent cycle and then pressurized with fresh CO (115 psia). The solution was then monitored by ^{31}P NMR for 2 days to ensure equilibration. The NMR spectra showed no change in the ratio of the two anions nor liberation of free P(pyrrolyl)$_3$.

A similar experiment was performed using 0.0453 g (0.0317 mmol) of [PPN][Rh(CO){P(pyrrolyl)$_3$}$_3$]·THF in 0.6 mL of THF. At 25 °C and 115 psia CO, a 33% equilibrium conversion of [Rh(CO)-{P(pyrrolyl)$_3$}$_3]^-$ to $[Rh(CO)_2${P(pyrrolyl)$_3$}$_2]^-$ and noncoordinated P(pyrrolyl)$_3$ was determined by ^{31}P NMR. The tube was then pressurized/vented several times with N_2 to remove CO. ^{31}P NMR showed gradual loss of free P(pyrrolyl)$_3$ and $[Rh(CO)_2${P(pyrrolyl)$_3$}$_2]^-$ and was accompanied by an increase in the concentration of $[Rh(CO){P(pyrrolyl)_3}_3]^-$. From these data the equilibrium constant for eq 9, $K = 0.19 \pm 0.05$, can be calculated.[43]

II. PPh$_3$. A similar experiment was performed using a *ca.* 20 mM solution of [PPN][Rh(CO)$_3$PPh$_3$] in THF, generated by the addition of PPh_3 to [PPN][Rh(CO)$_4$]. ^{31}P NMR spectroscopy at 75 psia CO showed complete (i.e., within detection limits) loss of $[Rh(CO)_3PPh_3]^-$ (δ 46.0, d, J_{Rh-P} = 159 Hz) and concomitant liberation of PPh_3 (δ −4.9).

X-ray Structural Analyses of Rh(CO)Cl(P(pyrrolyl)$_3$)$_2$, Rh(CO)-Cl(P(pyrrolidinyl)$_3$)$_2$, and [PPN][Rh(CO)(P(pyrrolyl)$_3$)$_3$]·THF. The same general procedure was followed for the crystallographic determinations of the molecular structures of Rh(CO)Cl(P(pyrrolyl)$_3$)$_2$, Rh(CO)Cl(P(pyrrolidinyl)$_3$)$_2$, and [PPN][Rh(CO)(P(pyrrolyl)$_3$)$_3$]·THF. The crystalline samples were sealed under nitrogen in capillary tubes and then optically aligned on the goniostat of a Siemens P4 automated X-ray diffractometer. The unit cell dimensions were initially determined by indexing a set of reflections whose angular coordinates were obtained with the automatic peak search routine provided with XSCANS. The systematic absences for Rh(CO)Cl(P(pyrrolyl)$_3$)$_2$ of {h 0 l}, l = 2*n* +1 and {0 k 0}, *k* = 2*n* +1 are uniquely consistent with the centrosymmetric monoclinic space group, $P2_1/c$. The crystallographic asymmetric unit of Rh(CO)Cl(P(pyrrolyl)$_3$)$_2$ further contains two independent molecules. The refined lattice parameters and other pertinent crystallographic information for these three compounds are summarized in Table 8.

Intensity data were measured with graphite-monochromated Mo-Kα radiation (λ = 0.71073 Å) and variable ω scans. The X-ray diffraction data for Rh(CO)Cl(P(pyrrolyl)$_3$)$_2$ and [PPN][Rh(CO)-(P(pyrrolyl)$_3$)$_3$]·THF were measured at ambient temperature, whereas the sample of Rh(CO)Cl(P(pyrrolidinyl)$_3$)$_2$ was cooled to 173 K in a nitrogen gas stream produced by a Siemens LT2 low-temperature attachment. Background counts were measured at the beginning and at the end of each scan with the crystal and counter kept stationary. The intensities of three standard reflections were measured periodically during data collection and gave no indication of sample movement.

(43) We have been unable to locate data on the solubility of CO in THF; to calculate equilibrium constants we used data available for 1,4-dioxane.[43a] At 296 K the solubility of CO in 1,4-dioxane is 5.7 mM/bar. Cargill, R. W. *Solubility Data Ser.* **1990**, *43 (Carbon Monoxide)*, 236−238.

The data were corrected for Lorentz-polarization and crystal decomposition (when appropriate) and symmetry-equivalent reflections were averaged.

Initial coordinates for the Rh and P atoms in $Rh(CO)Cl(P(pyrrolyl)_3)_2$ and $Rh(CO)Cl(P(pyrrolidinyl)_3)_2$ were interpolated from the sharpened Patterson map calculated with the structure solution software provided by SHELXTL IRIS.[44] All of the remaining non-hydrogen atoms were revealed by successive difference Fourier syntheses. Following anisotropic refinement of the non-hydrogen atoms, idealized positions for the hydrogen atoms were included as fixed contributions using a riding model. Full-matrix least-squares refinement,[44] based upon the minimization of $\sum w_i(|F_o| - |F_c|)^2$ with $w_i^{-1} = \sigma^2(F_o) + pF_o^2$, converged to give final discrepancy indices of $R(F_o) = 0.0644$, $R_w(F_o) = 0.0769$, and $\sigma_1 = 1.35$ for 4556 reflections with $F_o > 4.0\sigma(F_o)$ for $Rh(CO)Cl(P(pyrrolyl)_3)_2$ and $R(F_o) = 0.0328$, $R_w(F_o) = 0.0443$ and $\sigma_1 = 1.03$ for 4283 reflections with $F_o > 4.0\sigma(F_o)$ for $Rh(CO)Cl(P(pyrrolidinyl)_3)_2$. The discrepancy indices were calculated from the expressions $R(F_o) = \sum||F_o| - |F_c||/\sum|F_o|$ and $R_w(F_o) = \sum[(w_i)^{1/2}||F_o| - |F_c||]/\sum[(w_i)^{1/2}|F_o|]$ and the standard deviation of an observation of unit weight (GOF) equals $[\sum(w_i||F_o| - |F_c||^2)/(n - p)]^{1/2}$, where n is the number of observations and p is the number of parameters varied. Important bond distances and angles for the non-hydrogen atoms of $Rh(CO)Cl(P(pyrrolyl)_3)_2$ and $Rh(CO)Cl(P(pyrrolidinyl)_3)_2$ are listed in Tables 3 and 5, respectively.

The structure of $[PPN][Rh(CO)(P(pyrrolyl)_3)_3]\cdot THF$ was initially solved in the noncentrosymmetric space group P1 with the SHELXTL direct methods structure solution software. The fractional coordinates of the unique Rh atom were determined by translating the origin assigned for the phase determination from the midpoint of the coordinates of the two Rh atoms of the noncentrosymmetric cell to $x = 0$, $y = 0$, $z = 0$ and then translating the coordinates of these two Rh atoms relative to this new origin. Approximate coordinates for the remaining non-hydrogen atoms were revealed on subsequent Fourier maps calculated for the centrosymmetric $P\bar{1}$ cell. All hydrogen atoms were idealized with isotropic temperature factors set at 1.2 times that of the adjacent carbon.

Following the completion of the anisotropic refinement of the PPN^+ cation and the $[Rh(CO)(P(pyrrolyl)_3)_3]^-$ anion, it became apparent from the difference Fourier map that the crystal lattice also contained a disordered molecule of THF. This disorder was refined with a two-site model by varying the site occupancy factor (SOF) and restraining the corresponding 1,2 bond distances and the 1,3 intermolecular distances to be equivalent between the two sites for the disordered THF. The C−O and C−C distances were not constrained to idealized values but were allowed to vary within the defined restraints. The oxygen and carbon atom positions within each disordered THF site were refined anisotropically with idealized positions included for the eight hydrogen atoms. The refined value of SOF was 0.630(13) for atoms O2, C74, C75, C76, and C77. Full-matrix least-squares refinement, based upon the minimization of $\sum w_i(F_o^2 - F_c^2)^2$ with $w_i^{-1} = [\sigma^2(F_o^2) + (0.0413\ P)^2]$ where $P = (\mathrm{Max}(F_o^2,0) + 2F_c^2)/3$, was performed with SHELXL-93.[44] The final values of the discrepancy indices are provided in Table 1 and were calculated from the expressions $R1 = \sum||F_o| - |F_c||/\sum|F_o|$ and $wR2 = [\sum[w_i(F_o^2 - F_c^2)^2]/\sum[w_i(F_o^2)^2]]^{1/2}$. The standard deviation of an observation of unit weight (GOF) was computed from $[\sum[w_i(F_o^2 - F_c^2)^2]/(n - p)]^{1/2}$, where n is the number of reflections and p is the number of parameters varied. A listing of important interatomic distances and bond angles is provided in Table 7.

(44) Siemens Analytical X-ray Instruments, Inc.; Madison, WI. SHELXTL IRIS and SHELXL-93 are integrated software packages developed by G. M. Sheldrick of the University of Gottingen, Gottingen, Germany for the solution, refinement, and graphical display of molecular structures determined from single crystal X-ray diffraction data. These crystallographic computations were performed on a Silicon-Graphics Iris Indigo workstation.

Acknowledgment. Ms. T. L. Fortin is sincerely thanked for expert technical assistance. We would also like to thank Professors R. G. Bergman, J. R. Norton, C. R. Landis, and G. L. Geoffroy for insight and suggestions. Union Carbide Corporation is thanked for granting permission to publish these results. Financial support for the acquisition of a Siemens P4 X-ray diffractometer was provided by the Chemical Instrumentation Program of the National Science Foundation (Grant CHE 9120098).

Supporting Information Available: Tables of fractional atomic coordinates, complete bond distances and angles, and anisotropic thermal parameters for the complexes *trans*-$RhCl(CO)[P(pyrrolyl)_3]_2$, *trans*-$RhCl(CO)[P(pyrrolidinyl)_3]_2$, and $[PPN][Rh(CO)\{P(pyrrolyl)_3\}_3]$ (22 pages). This material is contained in many libraries on microfiche, immediately follows this article in the microfilm version of the journal, can be ordered from the ACS, and can be downloaded from the Internet; see any current masthead page for ordering information and Internet access instructions.

JA9506824